

RECEIVED: October 16, 2025

REVISED: February 10, 2026

ACCEPTED: March 23, 2026

PUBLISHED: June 10, 2026

# First measurement of the cross sections for $e^+e^- \rightarrow K^0 K^- \pi^+ J/\psi + \text{c.c.}$ at $\sqrt{s}$ from 4.396 to 4.951 GeV

---



## The BESIII collaboration

*Full author list at the end of the paper*

*E-mail:* [besiii-publications@ihep.ac.cn](mailto:besiii-publications@ihep.ac.cn)

**ABSTRACT:** Using  $e^+e^-$  collision data at 19 center-of-mass energies ranging from 4.396 to 4.951 GeV corresponding to a total integrated luminosity of  $8.86 \text{ fb}^{-1}$  collected by the BESIII detector, the process  $e^+e^- \rightarrow K^0 K^- \pi^+ J/\psi + \text{c.c.}$  is observed for the first time, with a statistical significance of  $9.4\sigma$  summing up all the data samples. Here, c.c. stands for the charge conjugated mode. For this process, the cross section and the upper limit at the 90% confidence level are reported at each of the 19 center-of-mass energies. No statistically significant vector structures are observed in the cross section line shape, nor as intermediate states of combinations of  $K\pi$ ,  $K\bar{K}$ ,  $K\bar{K}\pi$ ,  $KJ/\psi$ ,  $\pi J/\psi$ , and  $K\pi J/\psi$  seen at individual energy points or in the combined data sample.

**KEYWORDS:**  $e^+e^-$  Experiments, Exotics, Particle and Resonance Production, Quarkonium

**ARXIV EPRINT:** [2510.13274](https://arxiv.org/abs/2510.13274)

---

## Contents

<b>1</b>	<b>Introduction</b>	<b>1</b>
<b>2</b>	<b>BESIII detector and Monte Carlo simulation</b>	<b>2</b>
<b>3</b>	<b>Event reconstruction and selection</b>	<b>3</b>
3.1	Event reconstruction	3
3.2	Event selection	4
<b>4</b>	<b>Signal yields and cross sections</b>	<b>6</b>
4.1	Signal yield extraction	6
4.2	Cross section calculation	7
<b>5</b>	<b>Study of the possible intermediate states</b>	<b>10</b>
<b>6</b>	<b>Systematic uncertainties</b>	<b>12</b>
<b>7</b>	<b>Summary</b>	<b>14</b>
	<b>The BESIII collaboration</b>	<b>21</b>

---

## 1 Introduction

The charmonium-like states are promising candidates for exotic hadrons, such as tetraquarks, hadronic molecules, and hybrid mesons [1–6], since they show properties that are not compatible with the conventional  $c\bar{c}$  meson spectrum. These states provide valuable insight into non-perturbative quantum chromodynamics (QCD). The  $Y(4260)$ , the first observed  $Y$  state (also known as  $\psi(4230)$  [7]), was discovered by the BaBar experiment via the initial state radiation (ISR) process  $e^+e^- \rightarrow \gamma_{\text{ISR}}\pi^+\pi^-J/\psi$  [8]. Based on a series of cross section measurements for  $e^+e^- \rightarrow$  hadrons, including both hidden-charm and open-charm processes [9–27], several additional  $Y$  states have been observed. In addition, the excited charmonium states above  $4.6 \text{ GeV}/c^2$  predicted by the potential model, such as the  $5S$  and  $4D$  states, are not yet well established [28–32]. Experimentally, the  $Y(4660)$  (also known as  $\psi(4660)$  [7]) state was observed by the Belle experiment in the process  $e^+e^- \rightarrow \gamma_{\text{ISR}}\pi^+\pi^-\psi(3686)$  [12], confirmed by the BaBar [13] and BESIII [14] experiments. In addition, enhancements around  $4.6 \text{ GeV}$  are observed in the cross section line shapes for both the process  $e^+e^- \rightarrow D_s^+D_{s1}^-(2536)^- + \text{c.c.}$  and  $e^+e^- \rightarrow D_s^+D_{s2}^*(2573)^- + \text{c.c.}$  [21–23]. The  $Y(4500)$  and  $Y(4710)$  were discovered by the BESIII experiment in the cross-section line shape of the process  $e^+e^- \rightarrow K\bar{K}J/\psi$  [25–27], while the  $Y(4790)$  was observed in the process  $e^+e^- \rightarrow D_s^{*+}D_s^{*-}$  [24]. These observations imply some of  $Y$  states may harbor strange and charm quark-antiquark ( $s\bar{s}$  and  $c\bar{c}$ ) components within their wavefunction configurations. This motivates the investigation for the decay  $Y \rightarrow K^0K^-\pi^+J/\psi + \text{c.c.}$  as a natural extension of the current research.

Recently, the BESIII experiment reported the observation of a structure, denoted as  $Z_{cs}(3985)^-$  [33], with a significance of 5.3 standard deviation (denoted as  $5.3\sigma$ ), decaying into the  $(D_s^- D^{*0} + D_s^{*-} D^0)$  final state. Evidence for its neutral counterpart,  $Z_{cs}(3985)^0$  [34], has also been found in the  $(D_s^+ D^{*-} + D_s^{*+} D^-)$  system, with a significance of  $4.6\sigma$ . In addition, two charged  $Z_{cs}$  ( $Z_{cs}(4000)^+/Z_{cs}(4220)^+ \rightarrow K^+ J/\psi$ ) candidates were discovered in an amplitude analysis of the  $B^+ \rightarrow J/\psi \phi K^+$  decay at LHCb [35]. Discussions are ongoing about whether  $Z_{cs}(3985)^+$  and  $Z_{cs}(4000)^+$  represent the same state [36–44], as their masses are comparable, but their decay widths differ by nearly an order of magnitude. The  $Z_{cs}$  states have also been explored in the  $KJ/\psi$  and  $K\psi(3686)$  systems through the processes  $e^+e^- \rightarrow K\bar{K}J/\psi$  [27] and  $e^+e^- \rightarrow K\bar{K}\psi(3686)$  [45, 46] by the BESIII collaboration, but no significant signals were observed. Investigations of those  $Z_{cs}$  states through hidden-charm and open-strange channels play a crucial role in establishing their structural nature as molecular states, tetraquarks, or other exotic configurations [39, 44, 47–51]. The  $K^0 K^- \pi^+ J/\psi + \text{c.c.}$  final state also allows searching for  $Z_{cs}$  states with quantum numbers different from those of the observed states (such as  $J^P = 0^+$ ).

In addition, the authors of refs. [52, 53] predicted an excited  $K$  state with hidden charm by solving the Faddeev equations [54], denoted as  $K^*(4307)$ . Its mass and width are  $M = 4307 \text{ MeV}/c^2$  and  $\Gamma = 18 \text{ MeV}$ , and its quantum numbers are  $I(J^P) = 1/2(1^-)$ . The  $K^*(4307)$  is expected to decay predominantly to  $K^* J/\psi$ , and can be searched for via the process  $e^+e^- \rightarrow K^0 K^- \pi^+ J/\psi + \text{c.c.}$

In this paper, we report the first observation of the process  $e^+e^- \rightarrow K^0 K^- \pi^+ J/\psi + \text{c.c.}$  using data samples collected at 19 center-of-mass (c.m.) energies ( $\sqrt{s}$ ) from 4.396 to 4.951 GeV, corresponding to a total integrated luminosity of  $8.86 \text{ fb}^{-1}$ . The c.m. energy of the data sample is measured using the di-muon process for  $\sqrt{s} < 4.6 \text{ GeV}$  [55, 56] and the  $\Lambda_c \bar{\Lambda}_c$  pairs in  $e^+e^-$  annihilation for  $\sqrt{s} > 4.6 \text{ GeV}$  [57]. The integrated luminosities of these data samples are measured using large-angle Bhabha scattering sample [57, 58].

## 2 BESIII detector and Monte Carlo simulation

The BESIII detector [59] records symmetric  $e^+e^-$  collisions provided by the BEPCII storage ring [60] in the c.m. energy range from 1.84 to 4.95 GeV, with a peak luminosity of  $1.1 \times 10^{33} \text{ cm}^{-2}\text{s}^{-1}$  achieved at  $\sqrt{s} = 3.773 \text{ GeV}$ . BESIII has collected large data samples in this energy region [61–63]. The cylindrical core of the BESIII detector covers 93% of the full solid angle and consists of a helium-based multilayer drift chamber (MDC), a time-of-flight system (TOF), and a CsI (Tl) electromagnetic calorimeter (EMC), which are all enclosed in a superconducting solenoidal magnet providing a 1.0 T magnetic field. The solenoid is supported by an octagonal flux-return yoke with resistive plate counter muon identification modules interleaved with steel. The charged-particle momentum resolution at 1 GeV/ $c$  is 0.5%, and the  $dE/dx$  resolution is 6% for electrons from Bhabha scattering. The EMC measures photon energies with a resolution of 2.5% (5%) at 1 GeV in the barrel (end cap) region. The time resolution in the plastic scintillator TOF barrel region is 68 ps, while that in the end cap region was 110 ps. The end cap TOF system was upgraded in 2015 using multigap resistive plate chamber technology, providing a time resolution of 60 ps, which benefits 80% of the data used in this analysis [64–66].

Monte Carlo (MC) simulated data samples produced with a GEANT4-based [67, 68] software package, which includes the geometric description of the BESIII detector and the detector response, are used to determine detection efficiencies and to estimate backgrounds. The simulation models the beam energy spread and ISR in the  $e^+e^-$  annihilations with the generator KKMC [69, 70]. All particle decays are modelled with EVTGEN [71, 72] using branching fractions either taken from the Particle Data Group (PDG) [7], when available, or otherwise estimated with LUNDCHARM [73, 74]. Final state radiation (FSR) from charged final state particles is incorporated using the PHOTOS package [75]. The inclusive MC sample includes the production of open charm processes, the ISR production of vector charmonium(-like) states, and the continuum processes incorporated in KKMC [69, 70]. The signal process is not included in the inclusive MC samples. The inclusive MC samples, after removing processes including  $J/\psi \rightarrow l^+l^-$  ( $l = e, \mu$ ) in the final state, are denoted as “Bkg-Inc” in the following discussion.

The signal MC sample (denoted as PHSP MC) of  $e^+e^- \rightarrow K^0K^-\pi^+J/\psi + \text{c.c.}$ ,  $J/\psi \rightarrow l^+l^-$ ,  $K^0 \rightarrow K_S^0$  or  $K_L^0$ , is simulated at each c.m. energy point to determine the detection efficiency. In the signal MC simulation, the dressed cross section line shape of  $e^+e^- \rightarrow K^0K^-\pi^+J/\psi + \text{c.c.}$  measured in this study is used as input to calculate the ISR correction factor. To estimate the potential background contribution, additional MC samples (denoted as Bkg-Exc) of  $e^+e^- \rightarrow \pi\pi\psi(3686)$ ,  $K^+K^-J/\psi$ ,  $K_S^0K_S^0J/\psi$ ,  $\omega\chi_{c1,2}$ ,  $\phi\chi_{c0,1,2}$ ,  $\pi^+\pi^-X(3823)$ ,  $\eta^{(\prime)}J/\psi$ ,  $\psi(3686) \rightarrow \text{anything} + J/\psi$ ,  $X(3823) \rightarrow \gamma\chi_{c1}$ ,  $\chi_{c0,1,2} \rightarrow \gamma J/\psi$ ,  $\omega \rightarrow \pi^+\pi^-\pi^0$ ,  $\phi(K_S^0, \eta^{(\prime)}) \rightarrow \text{anything}$ ,  $\pi^0 \rightarrow \gamma\gamma$ , and  $J/\psi \rightarrow l^+l^-$  are generated, as these processes have similar final states with the signal processes. The cross sections of these processes are taken from the previous BESIII measurements [14, 20, 25–27, 76–79]. The Bkg-Inc and Bkg-Exc samples are used to study the sources of the background contributions and optimize the event selection criteria.

### 3 Event reconstruction and selection

To improve the detection efficiencies, both full and partial reconstruction methods are employed. The decay chain  $e^+e^- \rightarrow K_S^0K^-\pi^+J/\psi + \text{c.c.}$  is reconstructed using “full reconstruction”, “missing a  $K^\pm$  or  $\pi^\pm$ ”, and “missing a  $K_S^0$ ” methods. These result in the final states of  $K_S^0(\rightarrow \pi^+\pi^-)K^\pm\pi^\mp l^+l^-$ ,  $K_S^0(\rightarrow \pi^+\pi^-)\pi^\pm l^+l^-$  or  $K_S^0(\rightarrow \pi^+\pi^-)K^\pm l^+l^-$ , and  $K^\pm\pi^\mp l^+l^-$ , respectively. The process  $e^+e^- \rightarrow K_L^0K^-\pi^+J/\psi + \text{c.c.}$  is reconstructed using the “missing a  $K_L^0$ ” method, with the corresponding final states being  $K^\pm\pi^\mp l^+l^-$ . In the full text, “missing a  $K^0(\bar{K}^0)$ ” subsumes the methods of missing a  $K_L^0$  or a  $K_S^0$ , as they share the same final state. In the following sections, “full reconstruction”, “missing a  $K^\pm$  or  $\pi^\pm$ ”, and “missing a  $K^0(\bar{K}^0)$ ” selection methods are labeled as method I, method II, and method III, respectively. The following criteria will be used to identify the candidate events.

#### 3.1 Event reconstruction

Charged tracks detected in the MDC are required to be within a polar angle ( $\theta$ ) range of  $|\cos\theta| < 0.93$ , where  $\theta$  is defined with respect to the  $z$ -axis, which is the symmetry axis of the MDC. For charged tracks not originating from  $K_S^0$  decays, the distance of closest approach to the interaction point (IP) must be less than 10 cm along the  $z$ -axis,  $|V_z|$ , and less than

1 cm in the transverse plane,  $|V_{xy}|$ . Particle identification (PID) for charged tracks combines measurements of the energy deposited in the MDC and the flight time in the TOF to form likelihoods  $\mathcal{L}(h)$  ( $h = K, \pi$ ) for each hadron  $h$  hypothesis. Tracks are identified as kaons and pions by comparing the likelihoods for the kaon and pion hypotheses,  $\mathcal{L}(K) > \mathcal{L}(\pi)$  and  $\mathcal{L}(\pi) > \mathcal{L}(K)$ , respectively.

The  $K_S^0$  candidate is reconstructed from two oppositely charged tracks satisfying  $P < 1.0$  GeV/ $c$  and  $|V_z| < 20$  cm, where  $P$  represents the magnitude of the charged track's momentum. The two charged tracks are assigned as  $\pi^+\pi^-$  without imposing further PID criteria. They are constrained to originate from a common vertex and are required to have an invariant mass  $M_{\pi^+\pi^-}$  satisfying  $|M_{\pi^+\pi^-} - m_{K_S^0}| < 12$  MeV/ $c^2$ , where  $m_{K_S^0}$  is the  $K_S^0$  nominal mass [7]. The decay length of the  $K_S^0$  candidate is required to be greater than twice the vertex resolution. If more than one  $K_S^0$  are reconstructed in an event, the one with the smallest  $\chi^2$  is kept as the final  $K_S^0$  candidate, where  $\chi^2$  is derived from the secondary vertex fit of  $\pi^+\pi^-$ .

The other two charged tracks with momenta greater than 1.0 GeV/ $c$  and opposite charges are identified as the lepton pair from the  $J/\psi$  decay, while the remaining charged tracks are regarded as  $K^\pm$  or  $\pi^\pm$  according to the PID information. Electrons and muons are discriminated by requiring their deposited energies in the EMC (labeled as  $E(\text{EMC})$ ) to be greater than 1.0 GeV for electrons and less than 0.4 GeV for muons.

The selected lepton pair,  $K^\pm$ ,  $\pi^\pm$ , and  $K_S^0$  candidates in the event are combined to reconstruct the signal process. All charged tracks detected in the final states are used to perform a vertex fit to ensure they originate from the same vertex, and the  $\chi^2$  value of this fit is required to be less than 200.

## 3.2 Event selection

Depending on the number of  $K^\pm$ ,  $\pi^\pm$ , and  $K_S^0$ , the selection methods are divided into three categories: method I, II, and III. The selection criteria for each method are individually optimized using the Figure-of-Merit (FOM) defined as  $\varepsilon/(5/2 + \sqrt{B})$  [80], where  $\varepsilon$  is the detection efficiency of signal process, and  $B$  is the number of background events estimated by using the Bkg-Inc and Bkg-Exc samples (labelled as Bkg). The Bkg samples from various processes are normalized according to the corresponding cross sections and luminosities of data samples. Due to the limited data samples, the MC simulations from all the data samples are summed up in the optimization.

### 3.2.1 Method I-full reconstruction

If all the particles in the final state can be successfully reconstructed, the event is selected using the method I. A four-constraint (4C) kinematic fit is performed to ensure both energy and momentum conservation throughout the entire process, with a requirement of  $\chi_{4C}^2 < 200$ . To reduce the background processes due to  $\mu/\pi$  misidentification in the  $\mu^+\mu^-$  channel, the hit depth in MUC (Depth) is required to satisfy  $(\text{Depth}_{\mu^+} + \text{Depth}_{\mu^-}) > 75$  cm. After imposing these requirements, the invariant mass distribution of  $l^+l^-$  ( $M_{l^+l^-}$ ) is shown in figure 1 (left), where a clear  $J/\psi$  signal can be seen in data. The number of retained background events estimated by using the Bkg-Inc and Bkg-Exc samples is  $0.5 \pm 0.7$ .

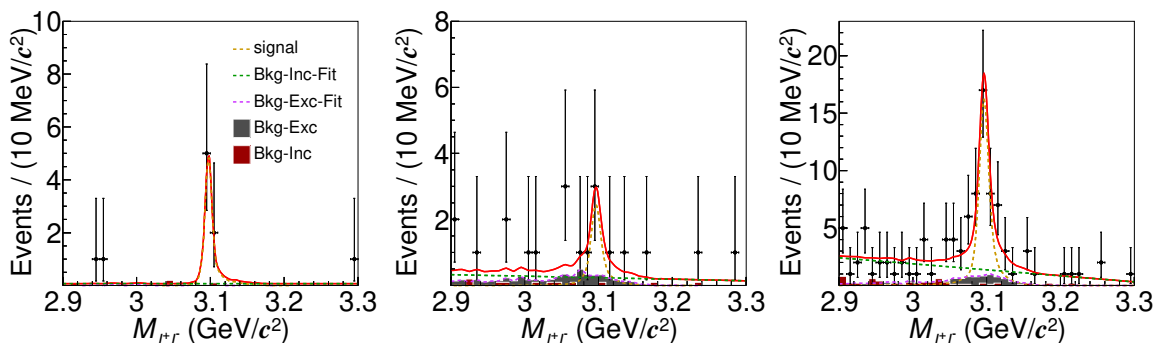


**Figure 1.** The  $M_{l+l-}$  distributions from “full reconstruction” (left), “missing a  $K^\pm$  or  $\pi^\pm$ ” (middle), and “missing a  $K^0(\bar{K}^0)$ ” (right) methods. The red and gray histograms represent the background contributions estimated from the Bkg-Inc and Bkg-Exc samples, respectively. The dots with error bars are the experimental data (summed over all data samples) and the red solid lines are the best fit result from a simultaneous fit.

### 3.2.2 Method II-missing a $K^\pm$ or $\pi^\pm$

If the event contains a  $\pi^\pm$  or  $K^\pm$ , at least one  $K_S^0$ , and a pair of leptons in the final state, the method II will be utilized. In this method, a one-constraint (1C) kinematic fit is applied, where the four-momenta of  $l^+$ ,  $l^-$ ,  $K^\pm$  or  $\pi^\pm$ ,  $K_S^0$  and a missing charged track are constrained to the initial four-momentum. The missing track’s three-momentum is unknown, but its mass is constrained to the mass of  $\pi^\pm$  or  $K^\pm$  taken from PDG [7]. If the reconstructed track is identified as  $\pi^\pm$ , then the missing one is assumed to be a  $K^\mp$ , and vice versa. In the  $e^+e^-$  mode, a two-dimensional optimization is performed on the distributions of  $E(\text{EMC})$  and  $\chi_{1\text{C}}^2$ , and the requirements are set to be  $\chi_{1\text{C}}^2 < 30$  and  $E(\text{EMC}) > 1.25$  GeV for at least one lepton to suppress background events. For the  $\mu^+\mu^-$  mode, the requirements of  $\chi_{1\text{C}}^2 < 20$  and  $(\text{Depth}_{\mu^+} + \text{Depth}_{\mu^-}) > 75$  cm are imposed, according to the optimization. After applying the aforementioned selection criteria, the invariant mass distribution of  $l^+l^-$  of the accepted candidates is depicted in figure 1 (middle). The total number of background events estimated from the Bkg-Inc and Bkg-Exc samples amounts to  $6.6 \pm 2.6$ .

### 3.2.3 Method III-missing a $K^0(\bar{K}^0)$

If the  $K^0(\bar{K}^0)$  oscillates to  $K_L^0$ , or  $K_S^0$  but failed to be reconstructed using the  $\pi^+\pi^-$  decay channel, and the numbers of  $K^\pm$ ,  $\pi^\pm$ , and lepton pair are all greater than 0, the method III is applied. In this method, a one-constraint (1C) kinematic fit is applied, where the four-momenta of  $K^\pm$ ,  $\pi^\pm$ ,  $l^+$ ,  $l^-$  and a missing  $K^0(\bar{K}^0)$  are constrained to the initial four-momentum. The three-momentum of missing  $K^0(\bar{K}^0)$  are unknown, but its mass is constrained at the nominal  $K^0(\bar{K}^0)$  mass [7]. If there are more than one  $K^\pm\pi^\mp$  combination in one event, the one yielding the smallest  $\chi_{1\text{C}}^2$  from the kinematic fit is preserved for subsequent analysis. To remove the background contributions from the QED processes ( $e^+e^- \rightarrow e^+e^-(n\gamma)$ ,  $e^+e^- \rightarrow \mu^+\mu^-(n\gamma)$ ,  $e^+e^- \rightarrow n\gamma$ ), the opening angles of  $e^\pm K^\mp$ ,  $e^\pm\pi^\mp$  and  $K^\pm\pi^\mp$  are required to satisfy  $|\cos\theta_{e^\pm K^\mp, e^\pm\pi^\mp, K^\pm\pi^\mp}| < 0.98$  for the  $e^+e^-$  mode. In addition, the criteria  $\chi_{1\text{C}}^2 < 30$  and  $E(\text{EMC}) > 1.3$  GeV for at least one lepton are applied. For the  $\mu^+\mu^-$  mode, the requirements  $\chi_{1\text{C}}^2 < 10$  and  $(\text{Depth}_{\mu^+} + \text{Depth}_{\mu^-}) > 80$  cm are used

to suppress background events. After the above selections, the distribution of  $M_{l+l^-}$  of the accepted candidates is shown in figure 1 (right), where the total number of background events estimated by using the Bkg-Inc and Bkg-Exc samples is  $17.5 \pm 4.2$ .

After all the event selection, the total number of background events estimated by using Bkg samples, summed over all the energy points and all the selection categories, is  $24.5 \pm 5.0$ . The fraction of the Bkg-Exc background events is about 66%, and that from the Bkg-Inc background events is about 34%. The Bkg-Inc background events are dominated by hadron processes and smoothly distributed in the  $M_{l+l^-}$  distribution. The  $M_{l+l^-}$  distributions from data and Bkg are also displayed for each energy point, as shown in figure 2.

## 4 Signal yields and cross sections

### 4.1 Signal yield extraction

A simultaneous unbinned maximum likelihood fit is performed to the  $M_{l+l^-}$  distributions from the three selection methods for all the data samples to estimate the significance of the signal process, as shown in figure 1. The signal probability density function in the fit is represented by the MC simulated  $J/\psi$  shape convolved with a Gaussian function, which accounts for the difference in mass resolution between data and MC simulation. Here, the signal MC shape is extracted from combined MC samples, where the signal MC simulations at each energy point are scaled according to the product of the luminosity and the detection efficiency, and then summed up. The parameters of the Gaussian function are obtained from the control sample  $e^+e^- \rightarrow \pi^+\pi^-\psi(3686)$ ,  $\psi(3686) \rightarrow \pi^+\pi^-J/\psi$ ,  $J/\psi \rightarrow l^+l^-$ , since the final state is similar to our signal process but with a larger statistics. In the simultaneous fit, the number of signal events ( $N_{\text{sig}}$ ) is a free parameter, while the signal yields from three selection methods are constraint to  $N_{\text{sig}}\mathcal{B}_i\epsilon_i$ , where  $\mathcal{B}_i$  and  $\epsilon_i$  denotes the branching fraction and detection efficiency of the  $i$ -th method, respectively. The background in the fit consists of two components. One is described by the Bkg-Exc MC shape, which is extracted from the dedicated MC simulations and normalized, with the number of events fixed to the estimated value. The remaining background component is described by a constant for the method I and a linear function for the method II and III, where the numbers of events are free parameters. The best fit result is shown in figure 1, and the total signal yield obtained from the fit is  $45.3 \pm 7.8$ . The statistical significance is evaluated using the formula  $\sqrt{2\ln(L_{\text{max}}/L_0)}/(\Delta\text{n.d.f} = 1)$ , where  $\ln L_{\text{max}}$  and  $\ln L_0$  are the logarithmic likelihood values with and without the signal component in the fits, and  $\Delta\text{n.d.f}$  denotes the change in the number of degrees of freedom. The signal significance is estimated to be  $9.4\sigma$ .

To extract the signal yield for each individual data sample, the  $M_{l+l^-}$  distributions from the three methods are combined and fitted due to limited data samples. In each fit, the signal shape is described by the corresponding signal MC shape convolved with a Gaussian function, where the mean and sigma values of the Gaussian function are taken from the control sample of  $e^+e^- \rightarrow \pi^+\pi^-\psi(3686)$ ,  $\psi(3686) \rightarrow \pi^+\pi^-J/\psi$ ,  $J/\psi \rightarrow l^+l^-$ . The smooth background contributions are modeled by a linear function, with parameters fixed to the values obtained from fitting the  $M_{l+l^-}$  distribution of all data samples that passed the three sets of selections. The numbers of signal and background events are free parameters. Other

background contributions estimated by the Bkg-Exc samples are included and fixed for both shape and yield in the fit. The best fit results are shown in figure 2. Due to the limited numbers of events that survived the final selection for the data samples taken at  $\sqrt{s} = 4467.06, 4527.14, 4574.50,$  and  $4611.86$  MeV, the fits on these samples are not feasible. Instead, the number of signal events is calculated using  $N_{\text{obs}} - N_{\text{Bkg}}$ . Here,  $N_{\text{obs}}$  denotes the number of observed events within the  $J/\psi$  signal region (3.08, 3.12) GeV/ $c^2$ , and  $N_{\text{Bkg}}$  represents the total background events in the same region, which include both  $J/\psi$  peaking-background and non- $J/\psi$  events. The peaking-background contribution is estimated using the Bkg-Exc samples within the  $J/\psi$  signal region, while the non- $J/\psi$  background is evaluated from the  $J/\psi$  sideband regions, defined as (3.02, 3.06) GeV/ $c^2$  and (3.14, 3.18) GeV/ $c^2$ . The contribution from the  $J/\psi$  sideband regions is scaled by 0.5, since the  $J/\psi$  sideband regions are two times as wide as the  $J/\psi$  signal region. The signal yields are summarized in table 1. The significance of the signal process for each data sample is estimated using the same method mentioned above, and the values are listed in table 1.

The statistical significance of the signal process for most data samples is below  $3\sigma$ , the upper limit of the number of signal events ( $N_{\text{sig}}^{\text{UL}}$ ) at 90% confidence level (C.L.) for these data samples is determined using a Bayesian method [81]. The  $M_{l+l-}$  distribution is fitted with the number of signal events fixed from 0 to  $n$  to obtain a series of likelihood values  $L$ , where  $n$  represents an extremely large value (40). The upper limit is determined by finding out the value of  $N_{\text{sig}}^{\text{UL}}$  corresponding to 90% of the likelihood profile with respect to the signal yield. The upper limits at 90% C.L. are listed in table 1. Assuming that the signal and background yields follow a Poisson distribution, the TROLKE package [82] in the CERNROOT framework [83] is used to determine the upper limit of the number of signal events at 90% C.L. for the data samples taken at  $\sqrt{s} = 4467.06, 4527.14, 4574.50,$  and  $4611.86$  MeV.

## 4.2 Cross section calculation

The Born cross section  $\sigma^{\text{Born}}$  of the signal process is calculated as:

$$\sigma^{\text{Born}}[e^+e^- \rightarrow K^0 K^- \pi^+ J/\psi + \text{c.c.}] = \frac{\sigma^{\text{dressed}}}{\frac{1}{|1-\Pi|^2}} = \frac{N_{\text{sig}}}{L_{\text{int}} \cdot (1 + \delta^r) \cdot \frac{1}{|1-\Pi|^2} \cdot \mathcal{B}(J/\psi \rightarrow l+l-) \cdot \varepsilon}, \quad (4.1)$$

where  $\sigma^{\text{dressed}}$  is the dressed cross section,  $N_{\text{sig}}$  is the signal yield,  $L_{\text{int}}$  is the integrated luminosity,  $\varepsilon$  is the detection efficiency, and  $\mathcal{B}$  is the branching fraction. The value of the vacuum polarization (VP) factor,  $\frac{1}{|1-\Pi|^2}$ , is calculated using a Fortran package provided by Fred Jegerlehner [84], where the corrections from leptonic and hadronic VP are included. The ISR correction factor,  $(1 + \delta^r)$ , is calculated following the procedure described in ref. [85]. The cross section line shape measured from this study is used as input for the ISR correction factor calculation. The obtained Born cross section at each energy point is listed in table 1. Given that no significant structure is observed in the dressed cross section line shape, the distribution is modeled using a continuum amplitude defined as:

$$n_0 \cdot PS(\sqrt{s})/s, \quad (4.2)$$

where  $n_0$  is free parameter, and  $PS(\sqrt{s})$  is the four-body decay  $[R(\sqrt{s}) \rightarrow K^0 K^- \pi^+ J/\psi + \text{c.c.}]$  phase space factor [7]. The  $1/s$  dependence follows the behavior of the total hadronic cross

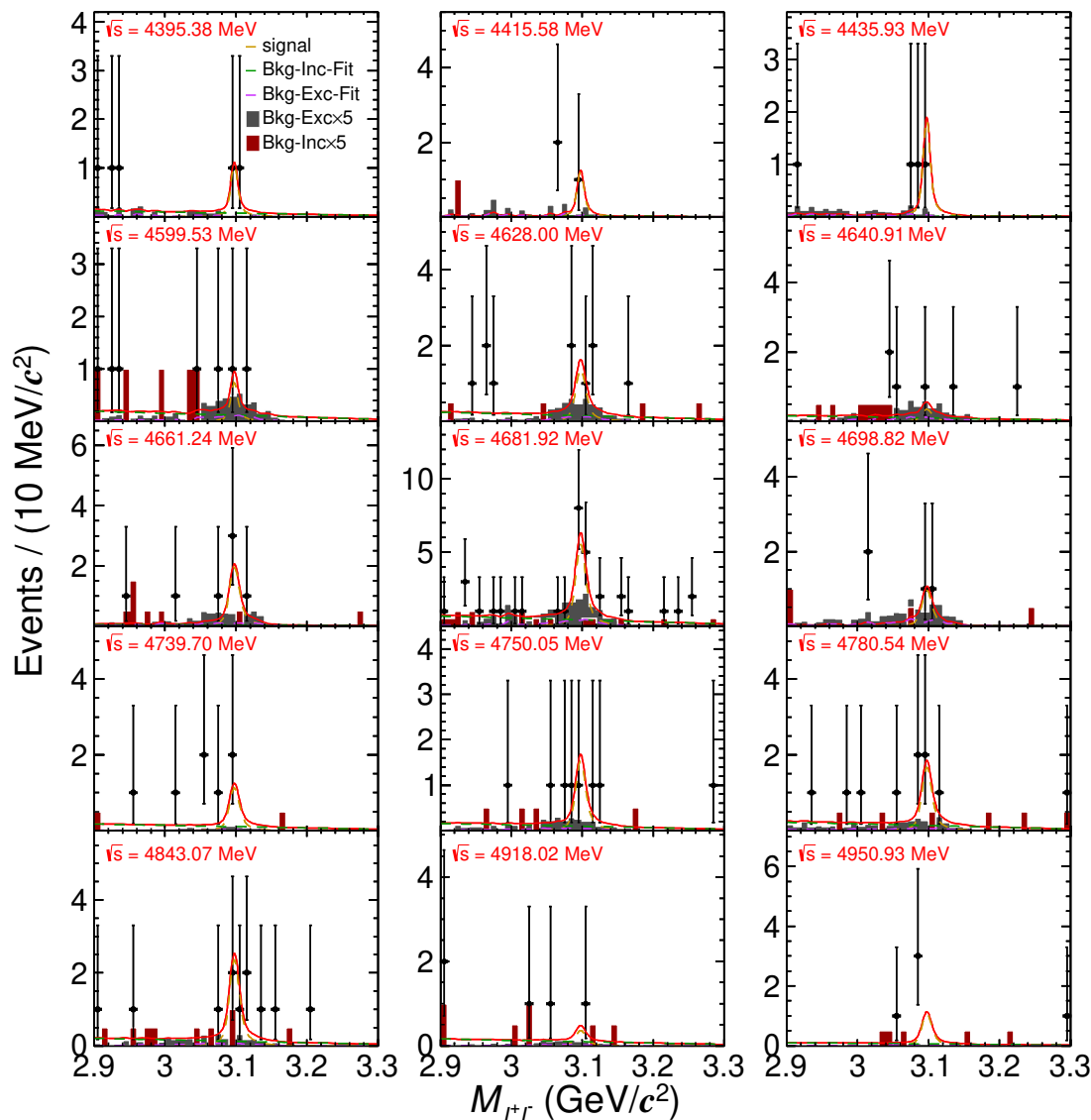


**Figure 2.** The fit results for data samples obtained by combining the three selection methods at different energy points. The red and gray histograms represent the background contributions estimated from the Bkg-Inc and Bkg-Exc samples, respectively. The dots with error bars are the data and the red solid lines are the best fit results. The Bkg events are scaled up by five to provide a clearer delineation of their contribution.

section on  $e^+e^-$  annihilation. The result of the fit to the dressed cross section is shown in figure 3.

The  $Y$  states, reported in the processes  $e^+e^- \rightarrow K^+K^-J/\psi$  and  $e^+e^- \rightarrow D_s^{*+}D_s^{*-}$ , are also searched for by including them in the fit. The cross section is fitted with a coherent sum of a Breit-Wigner (BW) function and the continuum amplitude:

$$\left| \frac{\sqrt{PS(\sqrt{s})} \cdot (\sqrt{12\pi}\Gamma_{ee}B\Gamma)}{\sqrt{PS(M)} \cdot (s - M^2 + iM\Gamma)} + \frac{n_0 \cdot \sqrt{PS(\sqrt{s})}}{\sqrt{s}} \cdot e^{i\phi} \right|^2, \quad (4.3)$$

$\sqrt{s}$ (MeV)	$\varepsilon_{K_S^0}$ (%)	$\varepsilon_{K_L^0}$ (%)	$N_{\text{sig}}$	$N_{\text{sig}}^{\text{UL}}$	$\frac{1+\delta^r}{ 1-\Pi ^2}$	$L_{\text{int}}$ (pb $^{-1}$ )	$\sigma^{\text{Born}}$ (pb)	$\sigma_{\text{UL}}^{\text{Born}}$ with sys. (pb)	Significance ( $\sigma$ )
4395.38	25.0 $\pm$ 0.1	15.9 $\pm$ 0.1	1.7 $^{+1.8}_{-1.1}$	5.2	0.850	507.8	0.16 $^{+0.17}_{-0.11}$ $\pm$ 0.01	0.5	1.9
4415.58	26.4 $\pm$ 0.1	17.0 $\pm$ 0.1	1.7 $^{+2.2}_{-1.2}$	5.7	0.804	1090.7	0.07 $^{+0.10}_{-0.05}$ $\pm$ 0.01	0.3	1.9
4435.93	27.5 $\pm$ 0.1	18.7 $\pm$ 0.1	2.7 $^{+2.1}_{-1.4}$	6.5	0.830	569.9	0.20 $^{+0.16}_{-0.11}$ $\pm$ 0.01	0.5	2.7
4467.06	26.1 $\pm$ 0.1	18.2 $\pm$ 0.1	0.0 $^{+1.1}_{-1.1}$	2.0	0.810	111.1	-0.01 $^{+0.48}_{-0.48}$ $\pm$ 0.01	0.8	—
4527.14	27.5 $\pm$ 0.1	20.2 $\pm$ 0.1	0.0 $^{+1.1}_{-1.1}$	2.0	0.822	112.1	-0.01 $^{+0.44}_{-0.44}$ $\pm$ 0.01	0.8	—
4574.50	28.5 $\pm$ 0.1	21.0 $\pm$ 0.1	-0.5 $^{+1.2}_{-1.2}$	1.6	0.829	48.9	-0.44 $^{+1.02}_{-0.96}$ $\pm$ 0.03	1.3	—
4599.53	31.9 $\pm$ 0.1	24.0 $\pm$ 0.1	1.2 $^{+1.9}_{-1.2}$	5.1	0.834	586.9	0.07 $^{+0.12}_{-0.07}$ $\pm$ 0.01	0.3	1.1
4611.86	28.2 $\pm$ 0.1	21.5 $\pm$ 0.1	0.9 $^{+2.3}_{-1.4}$	3.7	0.837	103.7	0.36 $^{+0.89}_{-0.55}$ $\pm$ 0.03	1.4	—
4628.00	31.9 $\pm$ 0.1	23.9 $\pm$ 0.1	2.9 $^{+2.7}_{-1.9}$	7.7	0.840	521.5	0.20 $^{+0.18}_{-0.13}$ $\pm$ 0.02	0.5	1.7
4640.91	32.1 $\pm$ 0.1	24.4 $\pm$ 0.1	0.7 $^{+1.6}_{-0.9}$	4.4	0.841	551.7	0.05 $^{+0.11}_{-0.06}$ $\pm$ 0.01	0.3	0.7
4661.24	32.4 $\pm$ 0.1	24.7 $\pm$ 0.1	4.3 $^{+2.7}_{-2.0}$	—	0.844	529.4	0.28 $^{+0.18}_{-0.13}$ $\pm$ 0.02	—	3.3
4681.92	32.5 $\pm$ 0.1	25.0 $\pm$ 0.1	12.2 $^{+4.5}_{-3.7}$	—	0.847	1667.4	0.25 $^{+0.09}_{-0.08}$ $\pm$ 0.02	—	4.7
4698.82	32.6 $\pm$ 0.1	25.3 $\pm$ 0.1	1.6 $^{+1.8}_{-1.2}$	5.3	0.849	535.5	0.11 $^{+0.12}_{-0.07}$ $\pm$ 0.01	0.3	1.8
4739.70	33.2 $\pm$ 0.1	25.7 $\pm$ 0.1	2.4 $^{+2.3}_{-1.5}$	6.9	0.853	163.9	0.50 $^{+0.48}_{-0.31}$ $\pm$ 0.03	1.4	2.1
4750.05	33.2 $\pm$ 0.1	25.6 $\pm$ 0.1	3.2 $^{+2.8}_{-2.1}$	8.1	0.854	366.6	0.29 $^{+0.26}_{-0.19}$ $\pm$ 0.02	0.7	1.9
4780.54	33.3 $\pm$ 0.1	25.8 $\pm$ 0.1	3.6 $^{+2.7}_{-2.0}$	8.4	0.858	511.5	0.23 $^{+0.17}_{-0.13}$ $\pm$ 0.02	0.5	2.4
4843.07	33.7 $\pm$ 0.1	26.8 $\pm$ 0.1	5.2 $^{+3.0}_{-2.3}$	—	0.865	525.2	0.32 $^{+0.19}_{-0.14}$ $\pm$ 0.03	—	3.1
4918.02	33.8 $\pm$ 0.1	26.9 $\pm$ 0.1	0.8 $^{+1.5}_{-0.8}$	4.1	0.873	207.8	0.12 $^{+0.23}_{-0.12}$ $\pm$ 0.01	0.6	1.0
4950.93	33.5 $\pm$ 0.1	27.0 $\pm$ 0.1	2.4 $^{+2.3}_{-1.7}$	6.7	0.875	159.3	0.49 $^{+0.46}_{-0.33}$ $\pm$ 0.04	1.3	1.5

**Table 1.** The Born cross section for different energy points, where the first and the second uncertainties are statistical and systematic, respectively. “ $\sigma_{\text{UL}}^{\text{Born}}$  with sys.” stands for the upper limits of the cross section with systematic uncertainties. “Significance” represents the statistical significance.  $L_{\text{int}}$  is the integrated luminosity.  $\varepsilon_{K_S^0}$  and  $\varepsilon_{K_L^0}$  represent the detection efficiency of the process  $e^+e^- \rightarrow K_S^0 K^- \pi^+ J/\psi + \text{c.c.}$  and  $e^+e^- \rightarrow K_L^0 K^- \pi^+ J/\psi + \text{c.c.}$ , respectively. Given the limited data samples for the data samples taken at  $\sqrt{s} = 4467.06, 4527.14, 4574.50,$  and  $4611.86$  MeV, the statistical significance is not evaluated. The signal significance exceeds  $3\sigma$  for the data samples taken at  $\sqrt{s} = 4661.24, 4681.92,$  and  $4843.07$  MeV.

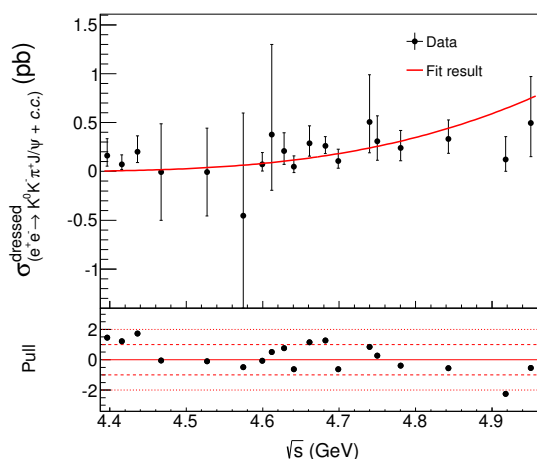


**Figure 3.** The dressed cross sections and fit results.

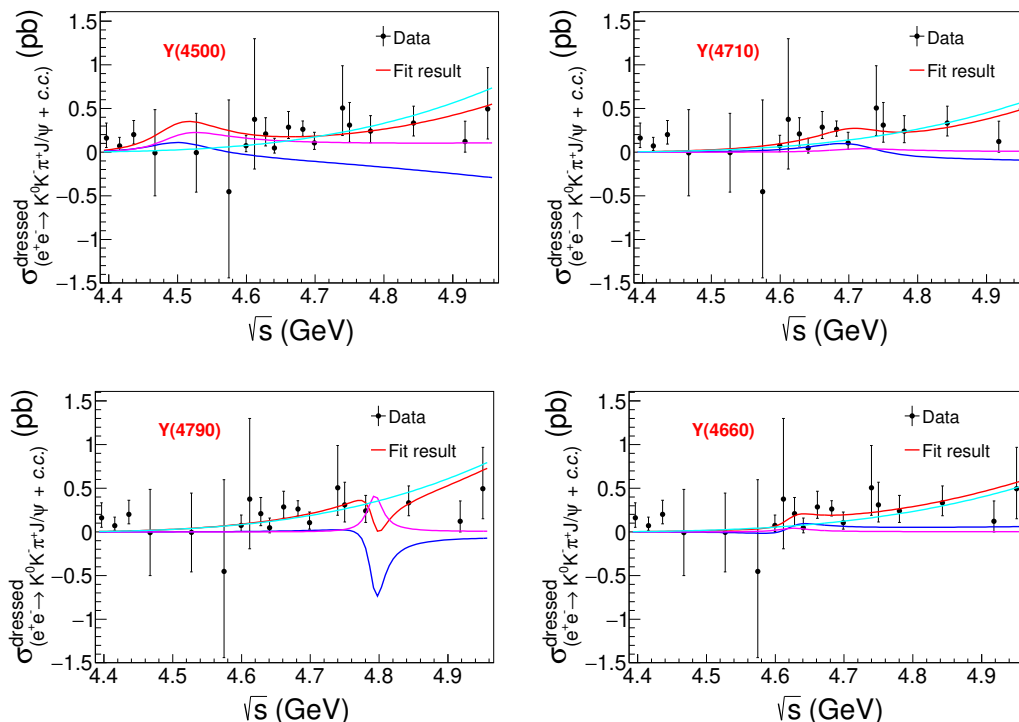


**Figure 4.** The dressed cross sections and fit results. The contributions from the BW, interference, and continuum term are represented by the pink, blue, and cyan curves, respectively.

where  $M$ ,  $\Gamma$ ,  $\Gamma_{ee}$ , and  $\mathcal{B}$  are the mass, full width, electronic width, and the branching fraction to  $K^0 K^- \pi^+ J/\psi + c.c.$  final state of each  $Y$  state, respectively. The BW parameters are fixed to that of  $Y(4500)$  ( $M = 4499.4 \text{ MeV}/c^2$ ,  $\Gamma = 124.0 \text{ MeV}$ ),  $Y(4710)$  ( $M = 4708.0 \text{ MeV}/c^2$ ,  $\Gamma = 126.0 \text{ MeV}$ ),  $Y(4790)$  ( $M = 4793.3 \text{ MeV}/c^2$ ,  $\Gamma = 27.1 \text{ MeV}$ ), or  $Y(4660)$  ( $M = 4623.0 \text{ MeV}/c^2$ ,  $\Gamma = 55.0 \text{ MeV}$ ). These values are taken from the measurements of the processes  $e^+e^- \rightarrow K^+K^- J/\psi$  [27],  $e^+e^- \rightarrow D_s^{*+}D_s^{*-}$  [24], and PDG [7]. The fit results are shown in figure 4, and the significance of the resonance contribution is less than  $2\sigma$  in all fits.

## 5 Study of the possible intermediate states

The selected events summed across all the data samples and selection methods are utilized to investigate the possible intermediate states in the  $K^{0,-}\pi^+ + c.c.$ ,  $K^0K^- + c.c.$ ,  $K^0K^- \pi^+ + c.c.$ ,  $\pi^\pm J/\psi$ ,  $K^{0,\pm}(\bar{K}^0)J/\psi$ ,  $K^{0,-}\pi^+ J/\psi + c.c.$  system, and the corresponding invariant mass distributions are illustrated in figure 5. The contribution from the  $J/\psi$  sideband regions is scaled by 0.5, a factor determined by fitting the  $M_{l+l^-}$  distribution from all data and calculating the ratio between the numbers of background events in the sideband and signal regions. The invariant mass of the  $K^{0,-}\pi^+ + c.c.$  ( $M_{K^{0,-}\pi^+ + c.c.}$ ) is utilized to investigate  $K^*$  states, encompassing both the  $K^0\pi^+ + c.c.$  and  $K^\pm\pi^\mp$  combinations, which results in each event being filled twice. The invariant mass of  $K^0K^- + c.c.$  ( $M_{K^0K^- + c.c.}$ ) is employed to study  $a_0(980)$  states. The invariant mass of  $K^0K^- \pi^+ + c.c.$  ( $M_{K^0K^- \pi^+ + c.c.}$ ) is applied to analyze the excited  $\eta$  states. The invariant mass of  $\pi^\pm J/\psi$  ( $M_{\pi^\pm J/\psi}$ ) is used to study possible  $Z_c$  states in the  $\pi^\pm J/\psi$  system. The resolution of  $M_{\pi^\pm J/\psi}$  is improved by utilizing the quantity

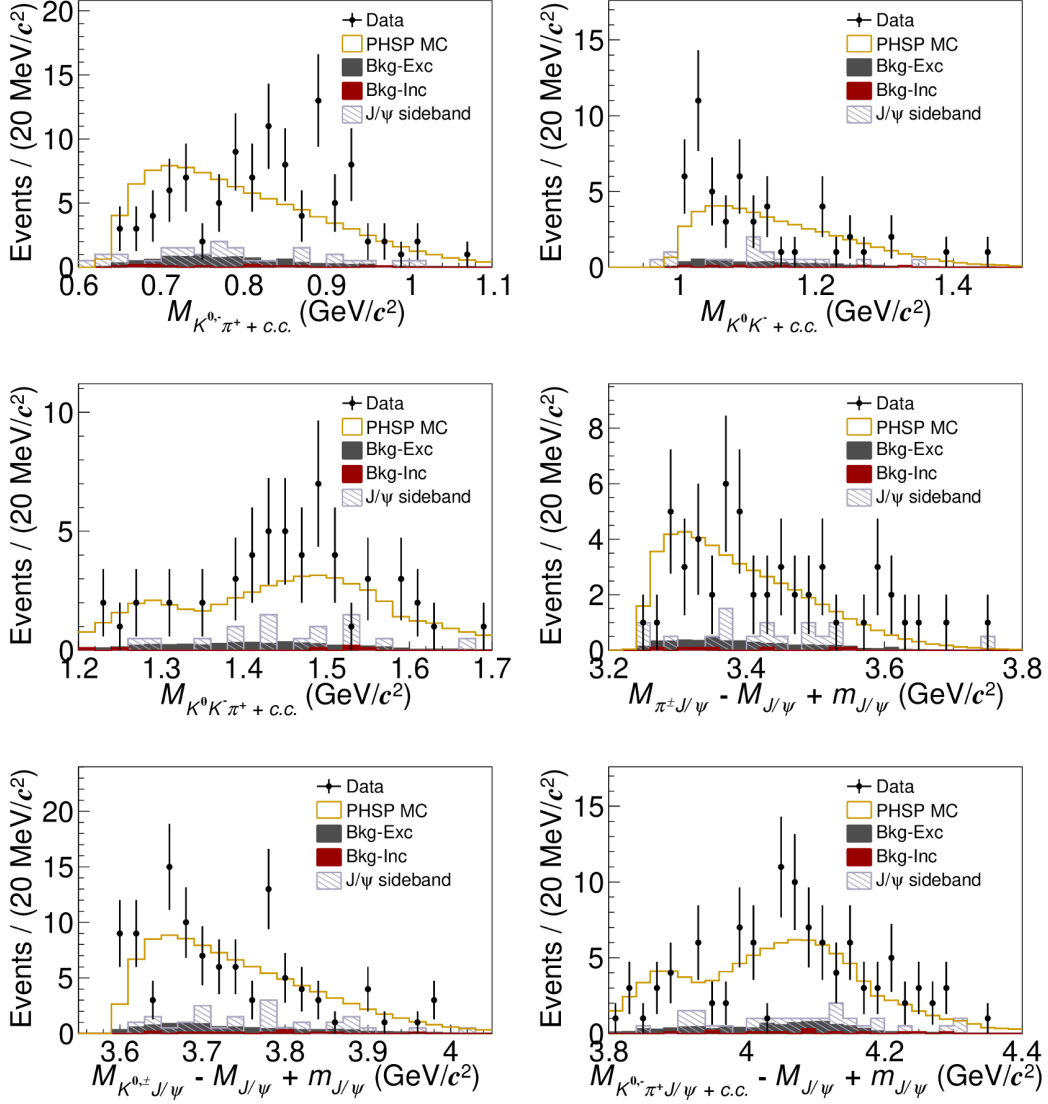


**Figure 5.** The comparison of the invariant mass spectra of  $K^0, -\pi^+ + c.c.$ ,  $K^0 K^- + c.c.$ ,  $K^0 K^- \pi^+ + c.c.$ ,  $\pi^\pm J/\psi$ ,  $K^{0,\pm}(\bar{K}^0)J/\psi$ , and  $K^0, -\pi^+ J/\psi + c.c.$  among data (dots with error bars, summing all data samples), PHSP MC, Bkg and  $J/\psi$  sideband. The signal MC samples at each energy point are scaled according to the product of the luminosity, the detection efficiency and the cross section, then added.

$M_{\pi^\pm J/\psi} - M_{J/\psi} + m_{J/\psi}$ , where  $M_{J/\psi}$  represents the invariant mass of the lepton pair, and  $m_{J/\psi}$  is the known mass as cited from the PDG [7]. The invariant mass of the  $K^{0,\pm}(\bar{K}^0)J/\psi$  ( $M_{K^{0,\pm}(\bar{K}^0)J/\psi}$ ) and  $K^0, -\pi^+ J/\psi + c.c.$  ( $M_{K^0, -\pi^+ J/\psi + c.c.}$ ) are employed to search for the  $Z_{cs}$  states. To improve the mass resolution, the requirements of  $M_{K^{0,\pm}(\bar{K}^0)J/\psi} - M_{J/\psi} + m_{J/\psi}$  and  $M_{K^0, -\pi^+ J/\psi + c.c.} - M_{J/\psi} + m_{J/\psi}$  are used instead of  $M_{K^{0,\pm}(\bar{K}^0)J/\psi}$  and  $M_{K^0, -\pi^+ J/\psi + c.c.}$ , respectively. Deviations from PHSP MC simulations are seen in the invariant mass distributions of  $K^0, -\pi^+ + c.c.$  and  $K^0 K^- + c.c.$  However, the statistical significances of the aforementioned intermediate states are all below  $3\sigma$ . Larger data samples are required to clarify the origin of these deviations.

$\sqrt{s}$ (MeV)	$L_{\text{int}}$	VP factor	Tracking	PID	Kfit	ISR-a	ISR-b	Br	MUC	MC model	Signal shape*	Bkg-a*	Bkg-b*	Total
4395.38	1.0	0.5	2.3	0.3	0.3	4.7	0.1	0.4	0.9	5.9	0.9	3.1	0.4	8.6
4415.58	1.0	0.5	2.3	0.3	0.4	1.8	0.1	0.4	0.9	2.0	0.9	3.1	0.4	5.0
4435.93	1.0	0.5	2.3	0.3	0.3	1.7	0.1	0.4	0.9	5.2	0.9	3.1	0.4	6.9
4467.06	1.0	0.5	2.3	0.3	0.7	1.0	0.1	0.4	0.9	9.6	—	—	—	10.0
4527.14	1.0	0.5	2.3	0.3	0.7	1.4	0.1	0.4	0.9	9.4	—	—	—	9.7
4574.50	1.0	0.5	2.3	0.3	0.8	1.8	0.1	0.4	0.9	7.1	—	—	—	7.8
4599.53	1.0	0.5	2.3	0.3	0.5	3.2	0.1	0.4	0.8	5.9	0.9	3.1	0.4	8.0
4611.86	0.6	0.5	2.3	0.3	0.7	2.1	0.1	0.4	1.8	6.0	—	—	—	7.1
4628.00	0.6	0.5	2.3	0.3	0.4	3.6	0.1	0.4	2.7	5.4	0.9	3.1	0.4	8.1
4640.91	0.6	0.5	2.3	0.3	0.4	3.8	0.1	0.4	2.7	5.5	0.9	3.1	0.4	8.3
4661.24	0.6	0.5	2.3	0.3	0.4	3.9	0.1	0.4	2.4	5.4	0.9	3.1	0.4	8.2
4681.92	0.6	0.5	2.3	0.3	0.4	3.7	0.1	0.4	2.1	5.8	0.9	3.1	0.4	8.2
4698.82	0.6	0.5	2.3	0.3	0.4	3.0	0.1	0.4	1.4	5.4	0.9	3.1	0.4	7.5
4739.70	0.6	0.5	2.3	0.3	0.3	1.8	0.1	0.4	0.6	4.9	0.9	3.1	0.4	6.6
4750.05	0.6	0.5	2.3	0.3	0.4	3.3	0.1	0.4	2.1	5.0	0.9	3.1	0.4	7.6
4780.54	0.6	0.5	2.3	0.3	0.5	6.4	0.1	0.4	0.9	4.5	0.9	3.1	0.4	8.9
4843.07	0.6	0.5	2.3	0.3	0.5	7.4	0.1	0.4	2.5	4.1	0.9	3.1	0.4	9.8
4918.02	0.6	0.5	2.3	0.3	0.4	6.1	0.1	0.4	0.6	4.0	0.9	3.1	0.4	8.4
4950.93	0.6	0.5	2.3	0.3	0.4	5.5	0.1	0.4	0.5	3.1	0.9	3.1	0.4	7.6

**Table 2.** Summary of the systematic uncertainties (in %) for the Born cross section measurements, where the sources marked with \* indicate additive uncertainties and the rest are multiplicative uncertainties. “ISR-a” and “ISR-b” refer to the systematic uncertainties arising from the parameterization form and the fit parameters of the cross section line shape, respectively. “Bkg-a” and “Bkg-b” denote the systematic uncertainties associated with the fixed Bkg-Exc background contribution and the background shapes, respectively. “Kinematic fit”, “Branching fraction”, and “MUC hit depth” are abbreviated as “Kfit”, “Br”, and “MUC”, respectively.

## 6 Systematic uncertainties

The systematic uncertainties on the Born cross section measurement are mainly caused by the integrated luminosity, tracking, PID, branching fraction, VP factor, ISR factor, kinematic fit, MUC hit depth, MC model, and fit procedure. The systematic uncertainties from the opening angles of  $e^\pm K^\mp$ ,  $e^\pm \pi^\mp$  and  $K^\pm \pi^\mp$  and  $E(\text{EMC})$  requirements are found to be negligible, estimated by the Barlow test [86]. The systematic uncertainties are summarized in table 2. The total systematic uncertainty is taken as a quadratic sum of each contribution. The systematic uncertainties in the determination of the upper limit of the cross section can be classified as either additive or multiplicative terms.

- *Integrated luminosity.* The integrated luminosities are measured using Bhabha events [57, 58], and the corresponding uncertainties are estimated to be 0.6% for  $\sqrt{s} > 4.6$  GeV and 1.0% for  $\sqrt{s} < 4.6$  GeV.
- *Tracking.* The systematic uncertainty of tracking is about 1.0% per track [87–89]. Since events with one missing track are included using the above mentioned selection method, the combined relative systematic uncertainty is calculated with

$$\left| \frac{\varepsilon \cdot \varepsilon + 2 \cdot \varepsilon(1 - \varepsilon)}{\varepsilon' \cdot \varepsilon' + 2 \cdot \varepsilon'(1 - \varepsilon')} - 1 \right| + 2\%, \quad (6.1)$$

where  $\varepsilon$  and  $\varepsilon' = \varepsilon \cdot (1 \pm 1\%)$  are the tracking efficiencies of MC simulation and data, respectively. The combined uncertainty is 2.3%.

- *PID*. This systematic uncertainty is calculated using the same method as used for tracking, and the corresponding uncertainty is assigned to be 1.0% per track [87–89].
- *Branching fraction*. The branching fractions of  $J/\psi \rightarrow e^+e^-$  and  $J/\psi \rightarrow \mu^+\mu^-$  are taken from the PDG [7], and they contribute an uncertainty of 0.4%.
- *VP factor*. The uncertainty in the vacuum polarization factor is 0.5%, taken from a QED calculation [90].
- *ISR factor*. To get the uncertainty from the parameterization form of the dressed cross section line shape, the fit formula is changed to  $|\sqrt{PS(\sqrt{s})/PS(M)} \cdot (\sqrt{12\pi\Gamma_{ee}\mathcal{B}\Gamma})/(s - M^2 + iM\Gamma)|^2$  and refit the dressed cross section. Here,  $M$  and  $\Gamma$  represent mass and total width, and are fixed to 4708.0 MeV/ $c^2$  and 126.0 MeV in the fit [27], respectively. Using the fitted curve to recalculate the ISR factor and detection efficiency, the difference from the nominal result is taken as systematic uncertainty. To get uncertainty from the fitted parameters, we change the parameter of  $n_0$  from eq. (4.2) within  $\pm 1\sigma$ , to reiterate and determine  $(1 + \delta^r) \cdot \varepsilon$  values. The largest difference on the resultant distribution of  $(1 + \delta^r) \cdot \varepsilon$  is taken as the systematic uncertainty, and the values are listed in table 2.
- *Kinematic fit*. The helix parameters of the charged tracks are corrected in MC simulation to improve the agreement of the  $\chi^2$  from the kinematic fit between data and simulation [91]. The systematic uncertainty from the kinematic fit is assigned as the difference in the efficiencies with and without this correction.
- *MUC hit depth*. The uncertainty from the MUC response is studied with a control sample of  $e^+e^- \rightarrow \mu^+\mu^-$  events. The difference in efficiency between the data and MC simulation is taken as the systematic uncertainty.
- *MC model*. To estimate the systematic uncertainty associated with the MC model, the processes  $e^+e^- \rightarrow K^0\bar{K}^{*0}(\rightarrow K^-\pi^+)J/\psi + \text{c.c.}$ ,  $e^+e^- \rightarrow K^{*+}(\rightarrow K^0\pi^+)K^-J/\psi + \text{c.c.}$ , and  $e^+e^- \rightarrow a_0^-(\rightarrow K^0K^-)\pi^+J/\psi + \text{c.c.}$  are generated. The larger difference in the detection efficiencies between MC samples with and without intermediate states is taken as the corresponding systematic uncertainty. For data samples with  $\sqrt{s} > 4527.14$  MeV, the difference between PHSP and  $e^+e^- \rightarrow K\bar{K}^*J/\psi + \text{c.c.}$  sample is taken, while for the remaining samples, the difference between PHSP and  $e^+e^- \rightarrow a_0^-\pi^+J/\psi + \text{c.c.}$  is used. The corresponding systematic uncertainties are listed in table 2.
- *Fit procedure*. To reduce statistical fluctuations, all data samples are combined to estimate the systematic uncertainty related to fit conditions. The fit procedure involves uncertainties from both the signal and background shapes. The signal MC shape convolved with a Gaussian function is used to describe the signal shape in the nominal fit. By varying the mean and standard deviation of the Gaussian function within one standard deviation and repeating the fit, the largest difference in the number of signal events is taken as the systematic uncertainty. For the background shapes, the parameters of the linear function are varied by  $\pm 1\sigma$ , and alternatively the background shape is changed from a first-order to a second-order polynomial function. The larger

difference obtained by varying the parameters of the linear function is taken as the systematic uncertainty. In the nominal fit, the number of Bkg-Exc events is fixed to  $\sum L_{\text{int}} \cdot \sigma_k \cdot \epsilon_k$ , where  $\sigma_k$  and  $\epsilon_k$  represent the cross section and detection efficiency of the  $k$ -th background process in the Bkg-Exc category. To estimate the associated systematic uncertainty, each  $\sigma_k$  is varied by its total uncertainty  $\Delta\sigma_k$  (i.e. changed by  $\pm 1\sigma$ ), and the fit is repeated. The largest resulting variation in the extracted signal yield is taken as the systematic uncertainty due to the fixed Bkg-Exc background contribution.

For the fitting method, the systematic uncertainties related to the fit procedure are treated as additive. The largest upper limit on the number of signal events, obtained from different fit conditions is taken. In addition, the multiplicative systematic uncertainty is incorporated by convolving the likelihood profile with respect to the signal yield corresponding to this most conservative result with a Gaussian function:

$$L'(x) = \int_0^1 L(x; N_{\text{sig}}\bar{\epsilon}/\hat{\epsilon}) \exp\left[-\frac{(\bar{\epsilon} - \hat{\epsilon})^2}{2\sigma_{\text{sys.}}^2}\right] d\bar{\epsilon},$$

where  $\hat{\epsilon}$  is the nominal average detection efficiency, and  $\sigma_{\text{sys.}}$  is the total multiplicative systematic uncertainty [81, 86].

For the counting method, the additive systematic uncertainties include the  $J/\psi$  signal region and the number of background events. The signal region is varied to (3.075, 3.115) or (3.085, 3.125) GeV/ $c^2$ , the sideband region is changed to (3.015, 3.055) and (3.135, 3.175) GeV/ $c^2$  or (3.025, 3.065) and (3.145, 3.185) GeV/ $c^2$ , and the number of Bkg-Exc events is changed with  $\pm 1\sigma$ , and the largest upper limit of the number of signal events is chosen. The multiplicative systematic uncertainties are considered in the calculations of the upper limit at 90% C.L. by using the TROLKE package [82] for the data samples taken at  $\sqrt{s} = 4467.06, 4527.14, 4574.50, \text{ and } 4611.86$  MeV.

## 7 Summary

In summary, based on the data samples taken at  $\sqrt{s}$  from 4395.4 to 4950.9 MeV, the  $e^+e^- \rightarrow K^0K^-\pi^+J/\psi + \text{c.c.}$  process is observed for the first time. Summing over all the data samples, the statistical significance is  $9.4\sigma$ . The upper limits at the 90% C.L. for the 16 c.m. energy points and the measurements for the 3 c.m. energy points on the cross section for the process  $e^+e^- \rightarrow K^0K^-\pi^+J/\psi + \text{c.c.}$  are reported for the first time. Additionally, no significant structure is observed in the cross section as a function of  $\sqrt{s}$ , and no obvious intermediate resonance states are detected among various combinations in the final state  $K^0K^-\pi^+J/\psi + \text{c.c.}$  The  $Z_{cs}$  states are investigated in the  $KJ/\psi$  and  $K\pi J/\psi$  systems, yet no significant signals are observed within the existing sensitivity limits of the data samples. More data are needed to search for the vector  $Y$ ,  $Z_c$ , and  $Z_{cs}$  states. This can be achieved with the upgraded BEPCII, which will plan to increase by a factor of three the luminosities at  $XYZ$  states energies [61].

## Acknowledgments

The BESIII Collaboration thanks the staff of BEPCII (<https://cstr.cn/31109.02.BEPC>) and the IHEP computing center for their strong support. This work is supported in part by the National Key R&D Program of China under Contracts Nos. 2025YFA1613900, 2023YFA1606000,

2023YFA1606704; the National Natural Science Foundation of China (NSFC) under Contracts Nos. 12375070, 11635010, 11935015, 11935016, 11935018, 12025502, 12035009, 12035013, 12061131003, 12192260, 12192261, 12192262, 12192263, 12192264, 12192265, 12221005, 12225509, 12235017, 12361141819; the Chinese Academy of Sciences (CAS) Large-Scale Scientific Facility Program; Joint Large Scale Scientific Facility Funds of the NSFC and CAS under Contracts Nos. U2032108; CAS under Contract No. YSBR-101; Shanghai Leading Talent Program of Eastern Talent Plan under Contract No. JLH5913002; Shanghai Top Talent Program of Eastern Talent Plan under Contract No. BJZH2025073; the 100 Talents Program of CAS; the Institute of Nuclear and Particle Physics (INPAC) and the Shanghai Key Laboratory for Particle Physics and Cosmology; the European Research Council (ERC) under Contract No. 758462; the German Research Foundation (DFG) under Contract No. FOR5327; the Istituto Nazionale di Fisica Nucleare, Italy; the Knut and Alice Wallenberg Foundation under Contracts Nos. 2021.0174 and 2021.0299; the Ministry of Development of Turkey under Contract No. DPT2006K-120470; the National Research Foundation of Korea under Contract No. NRF-2022R1A2C1092335; the National Science and Technology Fund of Mongolia; the Polish National Science Centre under Contract No. 2024/53/B/ST2/00975; the Science and Technology Facilities Council (STFC, United Kingdom); the Swedish Research Council under Contract No. 2019.04595; and the U.S. Department of Energy under Contract No. DE-FG02-05ER41374.

**Data Availability Statement.** This article has no associated data or the data will not be deposited.

**Code Availability Statement.** This article has no associated code or the code will not be deposited.

**Open Access.** This article is distributed under the terms of the Creative Commons Attribution License ([CC-BY4.0](https://creativecommons.org/licenses/by/4.0/)), which permits any use, distribution and reproduction in any medium, provided the original author(s) and source are credited.

## References

- [1] S.L. Olsen, T. Skwarnicki and D. Zieminska, *Non-Standard Heavy Mesons and Baryons, an Experimental Review*, *Rev. Mod. Phys.* **90** (2018) 015003 [[arXiv:1708.04012](https://arxiv.org/abs/1708.04012)] [[INSPIRE](#)].
- [2] C.-Z. Yuan and S.L. Olsen, *The BESIII Physics Programme*, *Nature Rev. Phys.* **1** (2019) 480 [[arXiv:2001.01164](https://arxiv.org/abs/2001.01164)] [[INSPIRE](#)].
- [3] N. Brambilla et al., *The XYZ states: experimental and theoretical status and perspectives*, *Phys. Rept.* **873** (2020) 1 [[arXiv:1907.07583](https://arxiv.org/abs/1907.07583)] [[INSPIRE](#)].
- [4] Y.-R. Liu et al., *Pentaquark and Tetraquark states*, *Prog. Part. Nucl. Phys.* **107** (2019) 237 [[arXiv:1903.11976](https://arxiv.org/abs/1903.11976)] [[INSPIRE](#)].
- [5] F.-K. Guo et al., *Hadronic molecules*, *Rev. Mod. Phys.* **90** (2018) 015004 [*Erratum ibid.* **94** (2022) 029901] [[arXiv:1705.00141](https://arxiv.org/abs/1705.00141)] [[INSPIRE](#)].
- [6] S. Godfrey and S.L. Olsen, *The Exotic XYZ Charmonium-like Mesons*, *Ann. Rev. Nucl. Part. Sci.* **58** (2008) 51 [[arXiv:0801.3867](https://arxiv.org/abs/0801.3867)] [[INSPIRE](#)].

- [7] PARTICLE DATA GROUP collaboration, *Review of Particle Physics*, *Phys. Rev. D* **110** (2024) 030001 [INSPIRE].
- [8] BABAR collaboration, *Observation of a Broad Structure in the  $\pi^+\pi^- J/\psi$  Mass Spectrum around  $4.26 \text{ GeV}/c^2$* , *Phys. Rev. Lett.* **95** (2005) 142001 [hep-ex/0506081] [INSPIRE].
- [9] BELLE collaboration, *Measurement of  $e^+e^- \rightarrow \pi^+\pi^- J/\psi$  cross-section via initial state radiation at Belle*, *Phys. Rev. Lett.* **99** (2007) 182004 [arXiv:0707.2541] [INSPIRE].
- [10] BESIII collaboration, *Precise Measurement of the  $e^+e^- \rightarrow \pi^+\pi^- J/\psi$  Cross Section at Center-of-Mass Energies from 3.77 to 4.60 GeV*, *Phys. Rev. Lett.* **118** (2017) 092001 [arXiv:1611.01317] [INSPIRE].
- [11] BESIII collaboration, *Study of the resonance structures in the process  $e^+e^- \rightarrow \pi^+\pi^- J/\psi$* , *Phys. Rev. D* **106** (2022) 072001 [arXiv:2206.08554] [INSPIRE].
- [12] BELLE collaboration, *Observation of Two Resonant Structures in  $e^+e^- \rightarrow \pi^+\pi^-\psi(2S)$  via Initial-State Radiation at Belle*, *Phys. Rev. Lett.* **99** (2007) 142002 [arXiv:0707.3699] [INSPIRE].
- [13] BABAR collaboration, *Study of the reaction  $e^+e^- \rightarrow \psi(2S)\pi^+\pi^-$  via initial-state radiation at BaBar*, *Phys. Rev. D* **89** (2014) 111103 [arXiv:1211.6271] [INSPIRE].
- [14] BESIII collaboration, *Cross section measurement of  $e^+e^- \rightarrow \pi^+\pi^-\psi(3686)$  from  $\sqrt{s} = 4.0076 \text{ GeV}$  to  $4.6984 \text{ GeV}$* , *Phys. Rev. D* **104** (2021) 052012 [arXiv:2107.09210] [INSPIRE].
- [15] BESIII collaboration, *Evidence of Two Resonant Structures in  $e^+e^- \rightarrow \pi^+\pi^- h_c$* , *Phys. Rev. Lett.* **118** (2017) 092002 [arXiv:1610.07044] [INSPIRE].
- [16] BESIII collaboration, *Cross section measurements of  $e^+e^- \rightarrow \omega\chi_{c0}$  from  $\sqrt{s} = 4.178$  to  $4.278 \text{ GeV}$* , *Phys. Rev. D* **99** (2019) 091103 [arXiv:1903.02359] [INSPIRE].
- [17] BESIII collaboration, *Evidence of a Resonant Structure in the  $e^+e^- \rightarrow \pi^+D^0D^{*-}$  Cross Section between 4.05 and 4.60 GeV*, *Phys. Rev. Lett.* **122** (2019) 102002 [arXiv:1808.02847] [INSPIRE].
- [18] BESIII collaboration, *Observation of Three Charmoniumlike States with  $J^{PC} = 1^{--}$  in  $e^+e^- \rightarrow D^{*0}D^{*-}\pi^+$* , *Phys. Rev. Lett.* **130** (2023) 121901 [arXiv:2301.07321] [INSPIRE].
- [19] BESIII collaboration, *Observation of the  $Y(4220)$  and  $Y(4390)$  in the process  $e^+e^- \rightarrow \eta J/\psi$* , *Phys. Rev. D* **102** (2020) 031101 [arXiv:2003.03705] [INSPIRE].
- [20] BESIII collaboration, *Measurement of  $e^+e^- \rightarrow \eta J/\psi$  cross section from  $\sqrt{s} = 3.808$  to  $4.951 \text{ GeV}$* , *Phys. Rev. D* **109** (2024) 092012 [arXiv:2310.03361] [INSPIRE].
- [21] BELLE collaboration, *Observation of a vector charmoniumlike state in  $e^+e^- \rightarrow D_s^+D_{s1}(2536)^- + c.c.$* , *Phys. Rev. D* **100** (2019) 111103 [arXiv:1911.00671] [INSPIRE].
- [22] BELLE collaboration, *Evidence for a vector charmoniumlike state in  $e^+e^- \rightarrow D_s^+D_{s2}^*(2573)^- + c.c.$* , *Phys. Rev. D* **101** (2020) 091101 [arXiv:2004.02404] [INSPIRE].
- [23] BESIII collaboration, *Study of the decay and production properties of  $D_{s1}(2536)$  and  $D_{s2}^*(2573)$* , *Phys. Rev. Lett.* **133** (2024) 171903 [arXiv:2407.07651] [INSPIRE].
- [24] BESIII collaboration, *Precise Measurement of the  $e^+e^- \rightarrow D_s^{*+}D_s^{*-}$  Cross Sections at Center-of-Mass Energies from Threshold to 4.95 GeV*, *Phys. Rev. Lett.* **131** (2023) 151903 [arXiv:2305.10789] [INSPIRE].
- [25] BESIII collaboration, *Observation of the  $Y(4230)$  and a new structure in  $e^+e^- \rightarrow K^+K^- J/\psi$* , *Chin. Phys. C* **46** (2022) 111002 [arXiv:2204.07800] [INSPIRE].

- [26] BESIII collaboration, *Observation of the  $Y(4230)$  and evidence for a new vector charmoniumlike state  $Y(4710)$  in  $e^+e^- \rightarrow K_S^0 K_S^0 J/\psi$* , *Phys. Rev. D* **107** (2023) 092005 [[arXiv:2211.08561](#)] [[INSPIRE](#)].
- [27] BESIII collaboration, *Observation of a Vector Charmoniumlike State at  $4.7\text{ GeV}/c^2$  and Search for  $Z_{cs}$  in  $e^+e^- \rightarrow K^+K^-J/\psi$* , *Phys. Rev. Lett.* **131** (2023) 211902 [[arXiv:2308.15362](#)] [[INSPIRE](#)].
- [28] N. Akbar, *Decay Properties of Conventional and Hybrid Charmonium Mesons*, *J. Korean Phys. Soc.* **77** (2020) 17 [[arXiv:2002.09566](#)] [[INSPIRE](#)].
- [29] R. Chaturvedi and A.K. Rai, *Charmonium spectroscopy motivated by general features of  $pNRQCD$* , *Int. J. Theor. Phys.* **59** (2020) 3508 [[arXiv:1910.06025](#)] [[INSPIRE](#)].
- [30] M.A. Sultan, N. Akbar, B. Masud and F. Akram, *Higher hybrid charmonia in an extended potential model*, *Phys. Rev. D* **90** (2014) 054001 [[arXiv:1403.6941](#)] [[INSPIRE](#)].
- [31] L.-C. Gui et al., *Strong decays of higher charmonium states into open-charm meson pairs*, *Phys. Rev. D* **98** (2018) 016010 [[arXiv:1801.08791](#)] [[INSPIRE](#)].
- [32] S. Kanwal, F. Akram, B. Masud and E.S. Swanson, *Charmonium spectrum in an unquenched quark model*, *Eur. Phys. J. A* **58** (2022) 219 [[arXiv:2211.08015](#)] [[INSPIRE](#)].
- [33] BESIII collaboration, *Observation of a Near-Threshold Structure in the  $K^+$  Recoil-Mass Spectra in  $e^+e^- \rightarrow K^+(D_s^-D^{*0} + D_s^{*-}D^0)$* , *Phys. Rev. Lett.* **126** (2021) 102001 [[arXiv:2011.07855](#)] [[INSPIRE](#)].
- [34] BESIII collaboration, *Evidence for a Neutral Near-Threshold Structure in the  $K_S^0$  Recoil-Mass Spectra in  $e^+e^- \rightarrow K_S^0 D_s^+ D^{*-}$  and  $e^+e^- \rightarrow K_S^0 D_s^{*+} D^-$* , *Phys. Rev. Lett.* **129** (2022) 112003 [[arXiv:2204.13703](#)] [[INSPIRE](#)].
- [35] LHCb collaboration, *Observation of New Resonances Decaying to  $J/\psi K^+$  and  $J/\psi \phi$* , *Phys. Rev. Lett.* **127** (2021) 082001 [[arXiv:2103.01803](#)] [[INSPIRE](#)].
- [36] L. Maiani, A.D. Polosa and V. Riquer, *The new resonances  $Z_{cs}(3985)$  and  $Z_{cs}(4003)$  (almost) fill two tetraquark nonets of broken  $SU(3)_f$* , *Sci. Bull.* **66** (2021) 1616 [[arXiv:2103.08331](#)] [[INSPIRE](#)].
- [37] P.-P. Shi, F. Huang and W.-L. Wang, *Hidden charm tetraquark states in a diquark model*, *Phys. Rev. D* **103** (2021) 094038 [[arXiv:2105.02397](#)] [[INSPIRE](#)].
- [38] J.F. Giron, R.F. Lebed and S.R. Martinez, *Spectrum of Hidden-Charm, Open-Strange Exotics in the Dynamical Diquark Model*, *Phys. Rev. D* **104** (2021) 054001 [[arXiv:2106.05883](#)] [[INSPIRE](#)].
- [39] Q.-N. Wang, W. Chen and H.-X. Chen, *Exotic  $\bar{D}_s^{(*)} D^{(*)}$  molecular states and  $sc\bar{c}$  tetraquark states with  $J^P = 0^+, 1^+, 2^{++}$* , *Chin. Phys. C* **45** (2021) 093102 [[arXiv:2011.10495](#)] [[INSPIRE](#)].
- [40] J.-B. Wang et al., *The low-lying hidden- and double-charm tetraquark states in a constituent quark model with Instanton-induced Interaction*, *Eur. Phys. J. C* **82** (2022) 721 [[arXiv:2204.13320](#)] [[INSPIRE](#)].
- [41] M. Karliner and J.L. Rosner, *Configuration mixing in strange tetraquarks  $Z_{cs}$* , *Phys. Rev. D* **104** (2021) 034033 [[arXiv:2107.04915](#)] [[INSPIRE](#)].
- [42] S. Han and L.-Y. Xiao, *Aspects of  $Z_{cs}(3985)$  and  $Z_{cs}(4000)$* , *Phys. Rev. D* **105** (2022) 054008 [[arXiv:2203.00168](#)] [[INSPIRE](#)].
- [43] L. Meng, B. Wang, G.-J. Wang and S.-L. Zhu, *Implications of the  $Z_{cs}(3985)$  and  $Z_{cs}(4000)$  as two different states*, *Sci. Bull.* **66** (2021) 2065 [[arXiv:2104.08469](#)] [[INSPIRE](#)].

- [44] Z.-G. Wang, *The decay widths of the  $Z_{cs}(3985/4000)$  based on rigorous quark-hadron duality*, *Chin. Phys. C* **46** (2022) 103106 [[arXiv:2205.03203](#)] [[INSPIRE](#)].
- [45] BESIII collaboration, *Measurement of the  $e^+e^- \rightarrow K^+K^-\psi(2S)$  Cross Section at Center-of-Mass Energies from 4.699 to 4.951 GeV and Search for  $Z_{cs}^\pm$  in the  $Z_{cs}^\pm \rightarrow K^\pm\psi(2S)$  Decay*, [arXiv:2407.20009](#) [[INSPIRE](#)].
- [46] BESIII collaboration, *Measurement of cross sections of  $e^+e^- \rightarrow K_S^0 K_S^0 \psi(3686)$  from  $\sqrt{s} = 4.682$  to 4.951 GeV*, *JHEP* **02** (2025) 120 [[arXiv:2411.15752](#)] [[INSPIRE](#)].
- [47] D.-Y. Chen, X. Liu and T. Matsuki, *Predictions of Charged Charmoniumlike Structures with Hidden-Charm and Open-Strange Channels*, *Phys. Rev. Lett.* **110** (2013) 232001 [[arXiv:1303.6842](#)] [[INSPIRE](#)].
- [48] J.M. Dias, X. Liu and M. Nielsen, *Prediction for the decay width of a charged state near the  $D_s \bar{D}^*/D_s^* \bar{D}$  threshold*, *Phys. Rev. D* **88** (2013) 096014 [[arXiv:1307.7100](#)] [[INSPIRE](#)].
- [49] M.B. Voloshin, *Strange hadrocharmonium*, *Phys. Lett. B* **798** (2019) 135022 [[arXiv:1901.01936](#)] [[INSPIRE](#)].
- [50] X. Cao and Z. Yang, *Hunting for the heavy quark spin symmetry partner of  $Z_{cs}$* , *Eur. Phys. J. C* **82** (2022) 161 [[arXiv:2110.09760](#)] [[INSPIRE](#)].
- [51] B.-D. Wan and C.-F. Qiao, *About the exotic structure of  $Z_{cs}$* , *Nucl. Phys. B* **968** (2021) 115450 [[arXiv:2011.08747](#)] [[INSPIRE](#)].
- [52] X.-L. Ren et al., *Heavy  $K^*(4307)$  meson with hidden charm*, in the proceedings of the 18th International Conference on Hadron Spectroscopy and Structure, Guilin, China, August 16–21 (2019) [[DOI:10.1142/9789811219313\\_0020](#)] [[arXiv:1912.04697](#)] [[INSPIRE](#)].
- [53] X.-L. Ren et al., *Heavy  $K^*(4307)$  Meson with Hidden Charm in the  $KD\bar{D}^*$  System*, *JPS Conf. Proc.* **26** (2019) 031006 [[INSPIRE](#)].
- [54] X.-L. Ren et al.,  *$K^*$  mesons with hidden charm arising from  $KX(3872)$  and  $KZ_c(3900)$  dynamics*, *Phys. Lett. B* **785** (2018) 112 [[arXiv:1805.08330](#)] [[INSPIRE](#)].
- [55] BESIII collaboration, *Measurements of the center-of-mass energies at BESIII via the di-muon process*, *Chin. Phys. C* **40** (2016) 063001 [[arXiv:1510.08654](#)] [[INSPIRE](#)].
- [56] BESIII collaboration, *Measurements of the center-of-mass energies of collisions at BESIII*, *Chin. Phys. C* **45** (2021) 103001 [[arXiv:2012.14750](#)] [[INSPIRE](#)].
- [57] BESIII collaboration, *Luminosities and energies of  $e^+e^-$  collision data taken between  $\sqrt{s} = 4.61$  GeV and 4.95 GeV at BESIII*, *Chin. Phys. C* **46** (2022) 113003 [[arXiv:2205.04809](#)] [[INSPIRE](#)].
- [58] BESIII collaboration, *Precision measurement of the integrated luminosity of the data taken by BESIII at center-of-mass energies between 3.810 GeV and 4.600 GeV*, *Chin. Phys. C* **39** (2015) 093001 [[arXiv:1503.03408](#)] [[INSPIRE](#)].
- [59] BESIII collaboration, *Design and Construction of the BESIII Detector*, *Nucl. Instrum. Meth. A* **614** (2010) 345 [[arXiv:0911.4960](#)] [[INSPIRE](#)].
- [60] C.H. Yu et al., *BEPCII Performance and Beam Dynamics Studies on Luminosity*, in the proceedings of the 7th International Particle Accelerator Conference, Busan, South Korea, May 08 (2016).
- [61] BESIII collaboration, *Future Physics Programme of BESIII*, *Chin. Phys. C* **44** (2020) 040001 [[arXiv:1912.05983](#)] [[INSPIRE](#)].

- [62] J. Lu, Y. Xiao and X. Ji, *Online monitoring of the center-of-mass energy from real data at BESIII*, *Radiat. Detect. Technol. Methods* **4** (2020) 337 [INSPIRE].
- [63] J.-W. Zhang et al., *Suppression of top-up injection backgrounds with offline event filter in the BESIII experiment*, *Radiat. Detect. Technol. Methods* **6** (2022) 289 [INSPIRE].
- [64] X. Li et al., *Study of MRPC technology for BESIII endcap-TOF upgrade*, *Radiat. Detect. Technol. Methods* **1** (2017) 13 [INSPIRE].
- [65] Y.-X. Guo et al., *The study of time calibration for upgraded end cap TOF of BESIII*, *Radiat. Detect. Technol. Methods* **1** (2017) 15 [INSPIRE].
- [66] P. Cao et al., *Design and construction of the new BESIII endcap Time-of-Flight system with MRPC Technology*, *Nucl. Instrum. Meth. A* **953** (2020) 163053 [INSPIRE].
- [67] GEANT4 collaboration, *GEANT4 — A Simulation Toolkit*, *Nucl. Instrum. Meth. A* **506** (2003) 250 [INSPIRE].
- [68] E.V. Abakumova et al., *The beam energy measurement system for the Beijing electron-positron collider*, *Nucl. Instrum. Meth. A* **659** (2011) 21 [arXiv:1109.5771] [INSPIRE].
- [69] S. Jadach, B.F.L. Ward and Z. Was, *The precision Monte Carlo event generator KK for two-fermion final states in  $e^+e^-$  collisions*, *Comput. Phys. Commun.* **130** (2000) 260 [hep-ph/9912214] [INSPIRE].
- [70] S. Jadach, B.F.L. Ward and Z. Was, *Coherent exclusive exponentiation for precision Monte Carlo calculations*, *Phys. Rev. D* **63** (2001) 113009 [hep-ph/0006359] [INSPIRE].
- [71] D.J. Lange, *The EvtGen particle decay simulation package*, *Nucl. Instrum. Meth. A* **462** (2001) 152 [INSPIRE].
- [72] R.-G. Ping, *Event generators at BESIII*, *Chin. Phys. C* **32** (2008) 599 [INSPIRE].
- [73] J.C. Chen et al., *Event generator for  $J/\psi$  and  $\psi(2S)$  decay*, *Phys. Rev. D* **62** (2000) 034003 [INSPIRE].
- [74] R.-L. Yang, R.-G. Ping and H. Chen, *Tuning and Validation of the Lundcharm Model with  $J/\psi$  Decays*, *Chin. Phys. Lett.* **31** (2014) 061301 [INSPIRE].
- [75] P. Golonka and Z. Was, *PHOTOS Monte Carlo: A precision tool for QED corrections in Z and W decays*, *Eur. Phys. J. C* **45** (2006) 97 [hep-ph/0506026] [INSPIRE].
- [76] BESIII collaboration, *Observation of Structures in the Processes  $e^+e^- \rightarrow \omega\chi_{c1}$  and  $\omega\chi_{c2}$* , *Phys. Rev. Lett.* **132** (2024) 161901 [arXiv:2401.14720] [INSPIRE].
- [77] BESIII collaboration, *Search for  $e^+e^- \rightarrow \phi\chi_{c0}$  and  $\phi\eta_{c2}(1D)$  at center-of-mass energies from 4.47 to 4.95 GeV*, *Phys. Rev. D* **111** (2025) 012016 [arXiv:2410.12620] [INSPIRE].
- [78] BESIII collaboration, *Study of  $e^+e^- \rightarrow \gamma\phi J/\psi$  from  $\sqrt{s} = 4.600$  to 4.951 GeV*, *JHEP* **01** (2023) 132.
- [79] BESIII collaboration, *Observation of Resonance Structures in  $e^+e^- \rightarrow \pi^+\pi^-\psi_2(3823)$  and Mass Measurement of  $\psi_2(3823)$* , *Phys. Rev. Lett.* **129** (2022) 102003 [arXiv:2203.05815] [INSPIRE].
- [80] G. Punzi, *Sensitivity of searches for new signals and its optimization*, *eConf C* **030908** (2003) MODT002 [physics/0308063] [INSPIRE].
- [81] J. Conrad, O. Botner, A. Hallgren and C. Perez de los Heros, *Including systematic uncertainties in confidence interval construction for Poisson statistics*, *Phys. Rev. D* **67** (2003) 012002 [hep-ex/0202013] [INSPIRE].
- [82] <https://root.cern.ch/root/html604/TRolke.html>.

- [83] <https://root.cern/manual>.
- [84] F. Jegerlehner, *Electroweak effective couplings for future precision experiments*, *Nuovo Cim. C* **034S1** (2011) 31 [[arXiv:1107.4683](#)] [[INSPIRE](#)].
- [85] W. Sun et al., *An iterative weighting method to apply ISR correction to  $e^+e^-$  hadronic cross-section measurements*, *Front. Phys. (Beijing)* **16** (2021) 64501 [[arXiv:2011.07889](#)] [[INSPIRE](#)].
- [86] O. Behnke, K. Kröniger, G. Schott and T. Schörner-Sadenius, *Data Analysis in High Energy Physics: A Practical Guide to Statistical Methods*, Wiley (2013) [[DOI:10.1002/9783527653416](#)].
- [87] W.-L. Yuan et al., *Study of tracking efficiency and its systematic uncertainty from  $J/\psi \rightarrow p\bar{p}\pi^+\pi^-$  at BESIII*, *Chin. Phys. C* **40** (2016) 026201 [[arXiv:1507.03453](#)] [[INSPIRE](#)].
- [88] BESIII collaboration, *Study of  $\psi(3686) \rightarrow \pi^0 h_c, h_c \rightarrow \gamma \eta_c$  via  $\eta_c$  exclusive decays*, *Phys. Rev. D* **86** (2012) 092009 [[arXiv:1209.4963](#)] [[INSPIRE](#)].
- [89] BESIII collaboration, *Study of  $\chi_{cJ}$  radiative decays into a vector meson*, *Phys. Rev. D* **83** (2011) 112005 [[arXiv:1103.5564](#)] [[INSPIRE](#)].
- [90] E.A. Kuraev and V.S. Fadin, *On Radiative Corrections to  $e^+e^-$  Single Photon Annihilation at High-Energy*, *Sov. J. Nucl. Phys.* **41** (1985) 466 [[INSPIRE](#)].
- [91] BESIII collaboration, *Search for hadronic transition  $\chi_{cJ} \rightarrow \eta_c \pi^+ \pi^-$  and observation of  $\chi_{cJ} \rightarrow K \bar{K} \pi \pi$* , *Phys. Rev. D* **87** (2013) 012002 [[arXiv:1208.4805](#)] [[INSPIRE](#)].

## The BESIII collaboration

M. Ablikim<sup>1</sup>, M.N. Achasov<sup>4,a</sup>, P. Adlarson<sup>77</sup>, X.C. Ai<sup>82</sup>, R. Aliberti<sup>36</sup>,  
A. Amoroso<sup>76a,76c</sup>, Q. An<sup>59,73,†</sup>, Y. Bai<sup>58</sup>, O. Bakina<sup>37</sup>, Y. Ban<sup>47,b</sup>, H.-R. Bao<sup>65</sup>,  
V. Batozskaya<sup>1,45</sup>, K. Begzsuren<sup>33</sup>, N. Berger<sup>36</sup>, M. Berlowski<sup>45</sup>, M. Bertani<sup>29a</sup>,  
D. Bettoni<sup>30a</sup>, F. Bianchi<sup>76a,76c</sup>, E. Bianco<sup>76a,76c</sup>, A. Bortone<sup>76a,76c</sup>, I. Boyko<sup>37</sup>,  
R.A. Briere<sup>5</sup>, A. Brueggemann<sup>70</sup>, H. Cai<sup>78</sup>, M.H. Cai<sup>39,c,d</sup>, X. Cai<sup>1,59</sup>, A. Calcaterra<sup>29a</sup>,  
G.F. Cao<sup>1,65</sup>, N. Cao<sup>1,65</sup>, S.A. Cetin<sup>63a</sup>, X.Y. Chai<sup>47,b</sup>, J.F. Chang<sup>1,59</sup>, G.R. Che<sup>44</sup>,  
Y.Z. Che<sup>1,59,65</sup>, C.H. Chen<sup>9</sup>, Chao Chen<sup>56</sup>, G. Chen<sup>1</sup>, H.S. Chen<sup>1,65</sup>, H.Y. Chen<sup>21</sup>,  
M.L. Chen<sup>1,59,65</sup>, S.J. Chen<sup>43</sup>, S.L. Chen<sup>46</sup>, S.M. Chen<sup>62</sup>, T. Chen<sup>1,65</sup>, X.R. Chen<sup>32,65</sup>,  
X.T. Chen<sup>1,65</sup>, X.Y. Chen<sup>12,e</sup>, Y.B. Chen<sup>1,59</sup>, Y.Q. Chen<sup>35</sup>, Y.Q. Chen<sup>16</sup>, Z.J. Chen<sup>26,f</sup>,  
Z.K. Chen<sup>60</sup>, J.C. Cheng<sup>46</sup>, S.K. Choi<sup>10</sup>, X. Chu<sup>12,e</sup>, G. Cibinetto<sup>30a</sup>, F. Cossio<sup>76c</sup>,  
J. Cottee-Meldrum<sup>64</sup>, J.J. Cui<sup>51</sup>, H.L. Dai<sup>1,59</sup>, J.P. Dai<sup>80</sup>, X.C. Dai<sup>62</sup>, A. Dbeysy<sup>19</sup>,  
R.E. de Boer<sup>3</sup>, F. De Mori<sup>76a,76c</sup>, D. Dedovich<sup>37</sup>, C.Q. Deng<sup>74</sup>, Z.Y. Deng<sup>1</sup>, A. Denig<sup>36</sup>,  
I. Denysenko<sup>37</sup>, M. Destefanis<sup>76a,76c</sup>, B. Ding<sup>1,68</sup>, X.X. Ding<sup>47,b</sup>, Y. Ding<sup>41</sup>, Y. Ding<sup>35</sup>,  
Y.X. Ding<sup>31</sup>, J. Dong<sup>1,59</sup>, L.Y. Dong<sup>1,65</sup>, M.Y. Dong<sup>1,59,65</sup>, X. Dong<sup>78</sup>, M.C. Du<sup>1</sup>,  
S.X. Du<sup>82</sup>, S.X. Du<sup>12,e</sup>, Y.Y. Duan<sup>56</sup>, Z.H. Duan<sup>43</sup>, P. Egorov<sup>37,g</sup>, G.F. Fan<sup>43</sup>,  
J.J. Fan<sup>20</sup>, Y.H. Fan<sup>46</sup>, J. Fang<sup>1,59</sup>, J. Fang<sup>60</sup>, S.S. Fang<sup>1,65</sup>, W.X. Fang<sup>1</sup>,  
Y.Q. Fang<sup>1,59</sup>, L. Fava<sup>76b,76c</sup>, F. Feldbauer<sup>3</sup>, G. Felici<sup>29a</sup>, C.Q. Feng<sup>59,73</sup>, J.H. Feng<sup>16</sup>,  
L. Feng<sup>39,c,d</sup>, Q.X. Feng<sup>39,c,d</sup>, Y.T. Feng<sup>59,73</sup>, M. Fritsch<sup>3</sup>, C.D. Fu<sup>1</sup>, J.L. Fu<sup>65</sup>,  
Y.W. Fu<sup>1,65</sup>, H. Gao<sup>65</sup>, Y. Gao<sup>59,73</sup>, Y.N. Gao<sup>47,b</sup>, Y.N. Gao<sup>20</sup>, Y.Y. Gao<sup>31</sup>,  
S. Garbolino<sup>76c</sup>, I. Garzia<sup>30a,30b</sup>, L. Ge<sup>58</sup>, P.T. Ge<sup>20</sup>, Z.W. Ge<sup>43</sup>, C. Geng<sup>60</sup>,  
E.M. Gersabeck<sup>69</sup>, A. Gilman<sup>71</sup>, K. Goetzen<sup>13</sup>, J.D. Gong<sup>35</sup>, L. Gong<sup>41</sup>, W.X. Gong<sup>1,59</sup>,  
W. Gradl<sup>36</sup>, S. Gramigna<sup>30a,30b</sup>, M. Greco<sup>76a,76c</sup>, M.H. Gu<sup>1,59</sup>, Y.T. Gu<sup>15</sup>,  
C.Y. Guan<sup>1,65</sup>, A.Q. Guo<sup>32</sup>, L.B. Guo<sup>42</sup>, M.J. Guo<sup>51</sup>, R.P. Guo<sup>50</sup>, Y.P. Guo<sup>12,e</sup>,  
A. Guskov<sup>37,g</sup>, J. Gutierrez<sup>28</sup>, K.L. Han<sup>65</sup>, T.T. Han<sup>1</sup>, F. Hanisch<sup>3</sup>, K.D. Hao<sup>59,73</sup>,  
X.Q. Hao<sup>20</sup>, F.A. Harris<sup>67</sup>, C.Z. He<sup>47,b</sup>, K.K. He<sup>56</sup>, K.L. He<sup>1,65</sup>, F.H. Heinsius<sup>3</sup>,  
C.H. Heinz<sup>36</sup>, Y.K. Heng<sup>1,59,65</sup>, C. Herold<sup>61</sup>, P.C. Hong<sup>35</sup>, G.Y. Hou<sup>1,65</sup>, X.T. Hou<sup>1,65</sup>,  
Y.R. Hou<sup>65</sup>, Z.L. Hou<sup>1</sup>, H.M. Hu<sup>1,65</sup>, J.F. Hu<sup>57,h</sup>, Q.P. Hu<sup>59,73</sup>, S.L. Hu<sup>12,e</sup>,  
T. Hu<sup>1,59,65</sup>, Y. Hu<sup>1</sup>, Z.M. Hu<sup>60</sup>, G.S. Huang<sup>59,73</sup>, K.X. Huang<sup>60</sup>, L.Q. Huang<sup>32,65</sup>,  
P. Huang<sup>43</sup>, X.T. Huang<sup>51</sup>, Y.P. Huang<sup>1</sup>, Y.S. Huang<sup>60</sup>, N. Hüsken<sup>36</sup>, T. Hussain<sup>75</sup>,  
N. in der Wiesche<sup>70</sup>, J. Jackson<sup>28</sup>, Q. Ji<sup>1</sup>, Q.P. Ji<sup>20</sup>, W. Ji<sup>1,65</sup>, X.B. Ji<sup>1,65</sup>, X.L. Ji<sup>1,59</sup>,  
Y.Y. Ji<sup>51</sup>, Z.K. Jia<sup>59,73</sup>, D. Jiang<sup>1,65</sup>, H.B. Jiang<sup>78</sup>, P.C. Jiang<sup>47,b</sup>, S.J. Jiang<sup>9</sup>,  
T.J. Jiang<sup>17</sup>, X.S. Jiang<sup>1,59,65</sup>, Y. Jiang<sup>65</sup>, J.B. Jiao<sup>51</sup>, J.K. Jiao<sup>35</sup>, Z. Jiao<sup>24</sup>, S. Jin<sup>43</sup>,  
Y. Jin<sup>68</sup>, M.Q. Jing<sup>1,65</sup>, X.M. Jing<sup>65</sup>, T. Johansson<sup>77</sup>, S. Kabana<sup>34</sup>,  
N. Kalantar-Nayestanaki<sup>66</sup>, X.L. Kang<sup>9</sup>, X.S. Kang<sup>41</sup>, M. Kavatsyuk<sup>66</sup>, B.C. Ke<sup>82</sup>,  
V. Khachatryan<sup>28</sup>, A. Khoukaz<sup>70</sup>, R. Kiuchi<sup>1</sup>, O.B. Kolcu<sup>63a</sup>, B. Kopf<sup>3</sup>, M. Kuessner<sup>3</sup>,  
W. Kühn<sup>38</sup>, X. Kui<sup>1,65</sup>, N. Kumar<sup>27</sup>, A. Kupsc<sup>45,77</sup>, Q. Lan<sup>74</sup>, W.N. Lan<sup>20</sup>,  
T.T. Lei<sup>59,73</sup>, M. Lellmann<sup>36</sup>, T. Lenz<sup>36</sup>, C. Li<sup>48</sup>, C. Li<sup>44</sup>, C.H. Li<sup>40</sup>, C.K. Li<sup>21</sup>,  
D.M. Li<sup>82</sup>, F. Li<sup>1,59</sup>, G. Li<sup>1</sup>, H.B. Li<sup>1,65</sup>, H.J. Li<sup>20</sup>, H.N. Li<sup>57,h</sup>, Hui Li<sup>44</sup>, J.R. Li<sup>62</sup>,  
J.S. Li<sup>60</sup>, K. Li<sup>1</sup>, K.L. Li<sup>20</sup>, K.L. Li<sup>39,c,d</sup>, L.J. Li<sup>1,65</sup>, Lei Li<sup>49</sup>, M.H. Li<sup>44</sup>,  
M.R. Li<sup>1,65</sup>, P.L. Li<sup>65</sup>, P.R. Li<sup>39,c,d</sup>, Q.M. Li<sup>1,65</sup>, Q.X. Li<sup>51</sup>, R. Li<sup>18,32</sup>, S.X. Li<sup>12</sup>,  
Shanshan Li<sup>26,f</sup>, T. Li<sup>51</sup>, T.Y. Li<sup>44</sup>, W.D. Li<sup>1,65</sup>, W.G. Li<sup>1,†</sup>, X. Li<sup>1,65</sup>, X.H. Li<sup>59,73</sup>,  
X.K. Li<sup>47,b</sup>, X.L. Li<sup>51</sup>, X.Y. Li<sup>1,8</sup>, X.Z. Li<sup>60</sup>, Y. Li<sup>20</sup>, Y.G. Li<sup>47,b</sup>, Y.P. Li<sup>35</sup>,

Z.J. Li [ID](#)<sup>60</sup>, Z.Y. Li [ID](#)<sup>80</sup>, C. Liang [ID](#)<sup>43</sup>, H. Liang [ID](#)<sup>59,73</sup>, Y.F. Liang [ID](#)<sup>55</sup>, Y.T. Liang [ID](#)<sup>32,65</sup>, G.R. Liao [ID](#)<sup>14</sup>, L.B. Liao [ID](#)<sup>60</sup>, M.H. Liao [ID](#)<sup>60</sup>, Y.P. Liao [ID](#)<sup>1,65</sup>, J. Libby [ID](#)<sup>27</sup>, A. Limphirat [ID](#)<sup>61</sup>, C.C. Lin [ID](#)<sup>56</sup>, D.X. Lin [ID](#)<sup>32,65</sup>, L.Q. Lin [ID](#)<sup>40</sup>, T. Lin [ID](#)<sup>1</sup>, B.J. Liu [ID](#)<sup>1</sup>, B.X. Liu [ID](#)<sup>78</sup>, C. Liu [ID](#)<sup>35</sup>, C.X. Liu [ID](#)<sup>1</sup>, F. Liu [ID](#)<sup>1</sup>, F.H. Liu [ID](#)<sup>54</sup>, Feng Liu [ID](#)<sup>6</sup>, G.M. Liu [ID](#)<sup>57,h</sup>, H.B. Liu [ID](#)<sup>15</sup>, H.H. Liu [ID](#)<sup>1</sup>, H.M. Liu [ID](#)<sup>1,65</sup>, Huihui Liu [ID](#)<sup>22</sup>, J.B. Liu [ID](#)<sup>59,73</sup>, J.J. Liu [ID](#)<sup>21</sup>, K. Liu [ID](#)<sup>39,c,d</sup>, K. Liu [ID](#)<sup>74</sup>, K.Y. Liu [ID](#)<sup>41</sup>, Ke Liu [ID](#)<sup>23</sup>, L.C. Liu [ID](#)<sup>44</sup>, Lu Liu [ID](#)<sup>44</sup>, M.H. Liu [ID](#)<sup>12,e</sup>, M.H. Liu [ID](#)<sup>35</sup>, P.L. Liu [ID](#)<sup>1</sup>, Q. Liu [ID](#)<sup>65</sup>, S.B. Liu [ID](#)<sup>59,73</sup>, T. Liu [ID](#)<sup>12,e</sup>, W.K. Liu [ID](#)<sup>44</sup>, W.M. Liu [ID](#)<sup>59,73</sup>, W.T. Liu [ID](#)<sup>40</sup>, X. Liu [ID](#)<sup>39,c,d</sup>, X. Liu [ID](#)<sup>40</sup>, X.K. Liu [ID](#)<sup>39,c,d</sup>, X.L. Liu [ID](#)<sup>12,e</sup>, X.Y. Liu [ID](#)<sup>78</sup>, Y. Liu [ID](#)<sup>39,c,d</sup>, Y. Liu [ID](#)<sup>82</sup>, Y. Liu [ID](#)<sup>82</sup>, Y.B. Liu [ID](#)<sup>44</sup>, Z.A. Liu [ID](#)<sup>1,59,65</sup>, Z.D. Liu [ID](#)<sup>9</sup>, Z.Q. Liu [ID](#)<sup>51</sup>, X.C. Lou [ID](#)<sup>1,59,65</sup>, F.X. Lu [ID](#)<sup>60</sup>, H.J. Lu [ID](#)<sup>24</sup>, J.G. Lu [ID](#)<sup>1,59</sup>, X.L. Lu [ID](#)<sup>16</sup>, Y. Lu [ID](#)<sup>7</sup>, Y.H. Lu [ID](#)<sup>1,65</sup>, Y.P. Lu [ID](#)<sup>1,59</sup>, Z.H. Lu [ID](#)<sup>1,65</sup>, C.L. Luo [ID](#)<sup>42</sup>, J.R. Luo [ID](#)<sup>60</sup>, J.S. Luo [ID](#)<sup>1,65</sup>, M.X. Luo <sup>81</sup>, T. Luo [ID](#)<sup>12,e</sup>, X.L. Luo [ID](#)<sup>1,59</sup>, Z.Y. Lv [ID](#)<sup>23</sup>, X.R. Lyu [ID](#)<sup>65,i</sup>, Y.F. Lyu [ID](#)<sup>44</sup>, Y.H. Lyu [ID](#)<sup>82</sup>, F.C. Ma [ID](#)<sup>41</sup>, H.L. Ma [ID](#)<sup>1</sup>, Heng Ma [ID](#)<sup>26,f</sup>, J.L. Ma [ID](#)<sup>1,65</sup>, L.L. Ma [ID](#)<sup>51</sup>, L.R. Ma [ID](#)<sup>68</sup>, Q.M. Ma [ID](#)<sup>1</sup>, R.Q. Ma [ID](#)<sup>1,65</sup>, R.Y. Ma [ID](#)<sup>20</sup>, T. Ma [ID](#)<sup>59,73</sup>, X.T. Ma [ID](#)<sup>1,65</sup>, X.Y. Ma [ID](#)<sup>1,59</sup>, Y.M. Ma [ID](#)<sup>32</sup>, F.E. Maas [ID](#)<sup>19</sup>, I. MacKay [ID](#)<sup>71</sup>, M. Maggiora [ID](#)<sup>76a,76c</sup>, S. Malde [ID](#)<sup>71</sup>, Q.A. Malik [ID](#)<sup>75</sup>, H.X. Mao [ID](#)<sup>39,c,d</sup>, Y.J. Mao [ID](#)<sup>47,b</sup>, Z.P. Mao [ID](#)<sup>1</sup>, S. Marcello [ID](#)<sup>76a,76c</sup>, A. Marshall [ID](#)<sup>64</sup>, F.M. Melendi [ID](#)<sup>30a,30b</sup>, Y.H. Meng [ID](#)<sup>65</sup>, Z.X. Meng [ID](#)<sup>68</sup>, G. Mezzadri [ID](#)<sup>30a</sup>, H. Miao [ID](#)<sup>1,65</sup>, T.J. Min [ID](#)<sup>43</sup>, R.E. Mitchell [ID](#)<sup>28</sup>, X.H. Mo [ID](#)<sup>1,59,65</sup>, B. Moses [ID](#)<sup>28</sup>, N.Yu. Muchnoi [ID](#)<sup>4,a</sup>, J. Muskalla [ID](#)<sup>36</sup>, Y. Nefedov [ID](#)<sup>37</sup>, F. Nerling [ID](#)<sup>19,j</sup>, L.S. Nie [ID](#)<sup>21</sup>, I.B. Nikolaev <sup>4,a</sup>, Z. Ning [ID](#)<sup>1,59</sup>, S. Nisar <sup>11,k</sup>, W.D. Niu [ID](#)<sup>12,e</sup>, C. Normand [ID](#)<sup>64</sup>, S.L. Olsen [ID](#)<sup>10,65</sup>, Q. Ouyang [ID](#)<sup>1,59,65</sup>, S. Pacetti [ID](#)<sup>29b,29c</sup>, X. Pan [ID](#)<sup>56</sup>, Y. Pan [ID](#)<sup>58</sup>, A. Pathak [ID](#)<sup>10</sup>, Y.P. Pei [ID](#)<sup>59,73</sup>, M. Pelizaeus [ID](#)<sup>3</sup>, H.P. Peng [ID](#)<sup>59,73</sup>, X.J. Peng [ID](#)<sup>39,c,d</sup>, K. Peters [ID](#)<sup>13,j</sup>, K. Petridis [ID](#)<sup>64</sup>, J.L. Ping [ID](#)<sup>42</sup>, R.G. Ping [ID](#)<sup>1,65</sup>, S. Plura [ID](#)<sup>36</sup>, V. Prasad [ID](#)<sup>35</sup>, F.Z. Qi [ID](#)<sup>1</sup>, H.R. Qi [ID](#)<sup>62</sup>, M. Qi [ID](#)<sup>43</sup>, S. Qian [ID](#)<sup>1,59</sup>, W.B. Qian [ID](#)<sup>65</sup>, C.F. Qiao [ID](#)<sup>65</sup>, J.H. Qiao [ID](#)<sup>20</sup>, J.J. Qin [ID](#)<sup>74</sup>, J.L. Qin [ID](#)<sup>56</sup>, L.Q. Qin [ID](#)<sup>14</sup>, L.Y. Qin [ID](#)<sup>59,73</sup>, P.B. Qin [ID](#)<sup>74</sup>, X.P. Qin [ID](#)<sup>12,e</sup>, X.P. Qin [ID](#)<sup>40</sup>, X.S. Qin [ID](#)<sup>51</sup>, Z.H. Qin [ID](#)<sup>1,59</sup>, J.F. Qiu [ID](#)<sup>1</sup>, Z.H. Qu [ID](#)<sup>74</sup>, J. Rademacker [ID](#)<sup>64</sup>, C.F. Redmer [ID](#)<sup>36</sup>, A. Rivetti [ID](#)<sup>76c</sup>, M. Rolo [ID](#)<sup>76c</sup>, G. Rong [ID](#)<sup>1,65</sup>, S.S. Rong [ID](#)<sup>1,65</sup>, F. Rosini [ID](#)<sup>29b,29c</sup>, Ch. Rosner [ID](#)<sup>19</sup>, M.Q. Ruan [ID](#)<sup>1,59</sup>, N. Salone [ID](#)<sup>45,l</sup>, A. Sarantsev [ID](#)<sup>37,m</sup>, Y. Schelhaas [ID](#)<sup>36</sup>, K. Schoenning [ID](#)<sup>77</sup>, M. Scodggio [ID](#)<sup>30a</sup>, K.Y. Shan [ID](#)<sup>12,e</sup>, W. Shan [ID](#)<sup>25</sup>, X.Y. Shan [ID](#)<sup>59,73</sup>, Z.J. Shang [ID](#)<sup>39,c,d</sup>, J.F. Shangguan [ID](#)<sup>17</sup>, L.G. Shao [ID](#)<sup>1,65</sup>, M. Shao [ID](#)<sup>59,73</sup>, C.P. Shen [ID](#)<sup>12,e</sup>, H.F. Shen [ID](#)<sup>1,8</sup>, W.H. Shen [ID](#)<sup>65</sup>, X.Y. Shen [ID](#)<sup>1,65</sup>, B.A. Shi [ID](#)<sup>65</sup>, H. Shi [ID](#)<sup>59,73</sup>, J.L. Shi [ID](#)<sup>12,e</sup>, J.Y. Shi [ID](#)<sup>1</sup>, S.Y. Shi [ID](#)<sup>74</sup>, X. Shi [ID](#)<sup>1,59</sup>, H.L. Song [ID](#)<sup>59,73</sup>, J.J. Song [ID](#)<sup>20</sup>, T.Z. Song [ID](#)<sup>60</sup>, W.M. Song [ID](#)<sup>35</sup>, Y.J. Song [ID](#)<sup>12,e</sup>, Y.X. Song [ID](#)<sup>47,b,m</sup>, Zirong Song [ID](#)<sup>26,f</sup>, S. Sosio [ID](#)<sup>76a,76c</sup>, S. Spataro [ID](#)<sup>76a,76c</sup>, S Stansilaus [ID](#)<sup>71</sup>, F. Stieler [ID](#)<sup>36</sup>, S.S. Su [ID](#)<sup>41</sup>, Y.J. Su [ID](#)<sup>65</sup>, G.B. Sun [ID](#)<sup>78</sup>, G.X. Sun [ID](#)<sup>1</sup>, H. Sun [ID](#)<sup>65</sup>, H.K. Sun [ID](#)<sup>1</sup>, J.F. Sun [ID](#)<sup>20</sup>, K. Sun [ID](#)<sup>62</sup>, L. Sun [ID](#)<sup>78</sup>, S.S. Sun [ID](#)<sup>1,65</sup>, T. Sun [ID](#)<sup>52,o</sup>, Y.C. Sun [ID](#)<sup>78</sup>, Y.H. Sun [ID](#)<sup>31</sup>, Y.J. Sun [ID](#)<sup>59,73</sup>, Y.Z. Sun [ID](#)<sup>1</sup>, Z.Q. Sun [ID](#)<sup>1,65</sup>, Z.T. Sun [ID](#)<sup>51</sup>, C.J. Tang <sup>55</sup>, G.Y. Tang [ID](#)<sup>1</sup>, J. Tang [ID](#)<sup>60</sup>, J.J. Tang [ID](#)<sup>59,73</sup>, L.F. Tang [ID](#)<sup>40</sup>, Y.A. Tang [ID](#)<sup>78</sup>, L.Y. Tao [ID](#)<sup>74</sup>, M. Tat [ID](#)<sup>71</sup>, J.X. Teng [ID](#)<sup>59,73</sup>, J.Y. Tian [ID](#)<sup>59,73</sup>, W.H. Tian [ID](#)<sup>60</sup>, Y. Tian [ID](#)<sup>32</sup>, Z.F. Tian [ID](#)<sup>78</sup>, I. Uman [ID](#)<sup>63b</sup>, B. Wang [ID](#)<sup>1</sup>, B. Wang [ID](#)<sup>60</sup>, Bo Wang [ID](#)<sup>59,73</sup>, C. Wang [ID](#)<sup>39,c,d</sup>, C. Wang [ID](#)<sup>20</sup>, Cong Wang [ID](#)<sup>23</sup>, D.Y. Wang [ID](#)<sup>47,b</sup>, H.J. Wang [ID](#)<sup>39,c,d</sup>, J.J. Wang [ID](#)<sup>78</sup>, K. Wang [ID](#)<sup>1,59</sup>, L.L. Wang [ID](#)<sup>1</sup>, L.W. Wang [ID](#)<sup>35</sup>, M. Wang [ID](#)<sup>51</sup>, M. Wang [ID](#)<sup>59,73</sup>, N.Y. Wang [ID](#)<sup>65</sup>, S. Wang [ID](#)<sup>12,e</sup>, T. Wang [ID](#)<sup>12,e</sup>, T.J. Wang [ID](#)<sup>44</sup>, W. Wang [ID](#)<sup>60</sup>, W. Wang [ID](#)<sup>74</sup>, W.P. Wang [ID](#)<sup>36</sup>, X. Wang [ID](#)<sup>47,b</sup>, X.F. Wang [ID](#)<sup>39,c,d</sup>, X.J. Wang [ID](#)<sup>40</sup>, X.L. Wang [ID](#)<sup>12,e</sup>, X.N. Wang [ID](#)<sup>1,65</sup>, Xin Wang [ID](#)<sup>26,f</sup>, Y. Wang [ID](#)<sup>62</sup>, Y.D. Wang [ID](#)<sup>46</sup>, Y.F. Wang [ID](#)<sup>1,8,65</sup>, Y.H. Wang [ID](#)<sup>39,c,d</sup>, Y.J. Wang [ID](#)<sup>59,73</sup>, Y.L. Wang [ID](#)<sup>20</sup>, Y.N. Wang [ID](#)<sup>78</sup>, Y.Q. Wang [ID](#)<sup>1</sup>, Yaqian Wang [ID](#)<sup>18</sup>, Yi Wang [ID](#)<sup>62</sup>,

Yuan Wang<sup>18,32</sup>, Z. Wang<sup>1,59</sup>, Z.L. Wang<sup>74</sup>, Z.L. Wang<sup>2</sup>, Z.Q. Wang<sup>12,e</sup>, Z.Y. Wang<sup>1,65</sup>, D.H. Wei<sup>14</sup>, H.R. Wei<sup>44</sup>, F. Weidner<sup>70</sup>, S.P. Wen<sup>1</sup>, Y.R. Wen<sup>40</sup>, U. Wiedner<sup>3</sup>, G. Wilkinson<sup>71</sup>, M. Wolke<sup>77</sup>, C. Wu<sup>40</sup>, J.F. Wu<sup>1,8</sup>, L.H. Wu<sup>1</sup>, L.J. Wu<sup>1,65</sup>, L.J. Wu<sup>20</sup>, Lianjie Wu<sup>20</sup>, S.G. Wu<sup>1,65</sup>, S.M. Wu<sup>65</sup>, X. Wu<sup>12,e</sup>, X.H. Wu<sup>35</sup>, Y.J. Wu<sup>32</sup>, Z. Wu<sup>1,59</sup>, L. Xia<sup>59,73</sup>, X.M. Xian<sup>40</sup>, B.H. Xiang<sup>1,65</sup>, D. Xiao<sup>39,c,d</sup>, G.Y. Xiao<sup>43</sup>, H. Xiao<sup>74</sup>, Y.L. Xiao<sup>12,e</sup>, Z.J. Xiao<sup>42</sup>, C. Xie<sup>43</sup>, K.J. Xie<sup>1,65</sup>, X.H. Xie<sup>47,b</sup>, Y. Xie<sup>51</sup>, Y.G. Xie<sup>1,59</sup>, Y.H. Xie<sup>6</sup>, Z.P. Xie<sup>59,73</sup>, T.Y. Xing<sup>1,65</sup>, C.F. Xu<sup>1,65</sup>, C.J. Xu<sup>60</sup>, G.F. Xu<sup>1</sup>, H.Y. Xu<sup>2,68</sup>, H.Y. Xu<sup>2</sup>, M. Xu<sup>59,73</sup>, Q.J. Xu<sup>17</sup>, Q.N. Xu<sup>31</sup>, T.D. Xu<sup>74</sup>, W. Xu<sup>1</sup>, W.L. Xu<sup>68</sup>, X.P. Xu<sup>56</sup>, Y. Xu<sup>41</sup>, Y. Xu<sup>12,e</sup>, Y.C. Xu<sup>79</sup>, Z.S. Xu<sup>65</sup>, F. Yan<sup>12,e</sup>, H.Y. Yan<sup>40</sup>, L. Yan<sup>12,e</sup>, W.B. Yan<sup>59,73</sup>, W.C. Yan<sup>82</sup>, W.H. Yan<sup>6</sup>, W.P. Yan<sup>20</sup>, X.Q. Yan<sup>1,65</sup>, H.J. Yang<sup>52,o</sup>, H.L. Yang<sup>35</sup>, H.X. Yang<sup>1</sup>, J.H. Yang<sup>43</sup>, R.J. Yang<sup>20</sup>, T. Yang<sup>1</sup>, Y. Yang<sup>12,e</sup>, Y.F. Yang<sup>44</sup>, Y.H. Yang<sup>43</sup>, Y.Q. Yang<sup>9</sup>, Y.X. Yang<sup>1,65</sup>, Y.Z. Yang<sup>20</sup>, M. Ye<sup>1,59</sup>, M.H. Ye<sup>8,†</sup>, Z.J. Ye<sup>57,h</sup>, Junhao Yin<sup>44</sup>, Z.Y. You<sup>60</sup>, B.X. Yu<sup>1,59,65</sup>, C.X. Yu<sup>44</sup>, G. Yu<sup>13</sup>, J.S. Yu<sup>26,f</sup>, L.W. Yu<sup>12,e</sup>, M.C. Yu<sup>41</sup>, T. Yu<sup>74</sup>, X.D. Yu<sup>47,b</sup>, Y.C. Yu<sup>82</sup>, C.Z. Yuan<sup>1,65</sup>, H. Yuan<sup>1,65</sup>, J. Yuan<sup>35</sup>, J. Yuan<sup>46</sup>, L. Yuan<sup>2</sup>, S.C. Yuan<sup>1,65</sup>, S.H. Yuan<sup>74</sup>, X.Q. Yuan<sup>1</sup>, Y. Yuan<sup>1,65</sup>, Z.Y. Yuan<sup>60</sup>, C.X. Yue<sup>40</sup>, Ying Yue<sup>20</sup>, A.A. Zafar<sup>75</sup>, S.H. Zeng<sup>64</sup>, X. Zeng<sup>12,e</sup>, Y. Zeng<sup>26,f</sup>, Y.J. Zeng<sup>60</sup>, Y.J. Zeng<sup>1,65</sup>, X.Y. Zhai<sup>35</sup>, Y.H. Zhan<sup>60</sup>, Zhang<sup>71</sup>, A.Q. Zhang<sup>1,65</sup>, B.L. Zhang<sup>1,65</sup>, B.X. Zhang<sup>1</sup>, D.H. Zhang<sup>44</sup>, G.Y. Zhang<sup>20</sup>, G.Y. Zhang<sup>1,65</sup>, H. Zhang<sup>59,73</sup>, H. Zhang<sup>82</sup>, H.C. Zhang<sup>1,59,65</sup>, H.H. Zhang<sup>60</sup>, H.Q. Zhang<sup>1,59,65</sup>, H.R. Zhang<sup>59,73</sup>, H.Y. Zhang<sup>1,59</sup>, J. Zhang<sup>82</sup>, J. Zhang<sup>60</sup>, J.J. Zhang<sup>53</sup>, J.L. Zhang<sup>21</sup>, J.Q. Zhang<sup>42</sup>, J.S. Zhang<sup>12,e</sup>, J.W. Zhang<sup>1,59,65</sup>, J.Y. Zhang<sup>1</sup>, J.Z. Zhang<sup>1,65</sup>, Jianyu Zhang<sup>65</sup>, L.M. Zhang<sup>62</sup>, Lei Zhang<sup>43</sup>, N. Zhang<sup>82</sup>, P. Zhang<sup>1,8</sup>, Q. Zhang<sup>20</sup>, Q.Y. Zhang<sup>35</sup>, R.Y. Zhang<sup>39,c,d</sup>, S.H. Zhang<sup>1,65</sup>, Shulei Zhang<sup>26,f</sup>, X.M. Zhang<sup>1</sup>, X.Y. Zhang<sup>41</sup>, X.Y. Zhang<sup>51</sup>, Y. Zhang<sup>1</sup>, Y. Zhang<sup>74</sup>, Y.H. Zhang<sup>1,59</sup>, Y.M. Zhang<sup>40</sup>, Y.P. Zhang<sup>59,73</sup>, Y.T. Zhang<sup>82</sup>, Z.D. Zhang<sup>1</sup>, Z.H. Zhang<sup>1</sup>, Z.L. Zhang<sup>35</sup>, Z.L. Zhang<sup>56</sup>, Z.X. Zhang<sup>20</sup>, Z.Y. Zhang<sup>78</sup>, Z.Y. Zhang<sup>44</sup>, Z.Z. Zhang<sup>46</sup>, Zh.Zh. Zhang<sup>20</sup>, G. Zhao<sup>1</sup>, J.Y. Zhao<sup>1,65</sup>, J.Z. Zhao<sup>1,59</sup>, L. Zhao<sup>1</sup>, L. Zhao<sup>59,73</sup>, M.G. Zhao<sup>44</sup>, N. Zhao<sup>80</sup>, R.P. Zhao<sup>65</sup>, S.J. Zhao<sup>82</sup>, Y.B. Zhao<sup>1,59</sup>, Y.L. Zhao<sup>56</sup>, Y.X. Zhao<sup>32,65</sup>, Z.G. Zhao<sup>59,73</sup>, A. Zhemchugov<sup>37,g</sup>, B. Zheng<sup>74</sup>, B.M. Zheng<sup>35</sup>, J.P. Zheng<sup>1,59</sup>, W.J. Zheng<sup>1,65</sup>, X.R. Zheng<sup>20</sup>, Y.H. Zheng<sup>65,i</sup>, B. Zhong<sup>42</sup>, C. Zhong<sup>20</sup>, H. Zhou<sup>36,51,p</sup>, J.Q. Zhou<sup>35</sup>, J.Y. Zhou<sup>35</sup>, S. Zhou<sup>6</sup>, X. Zhou<sup>78</sup>, X.K. Zhou<sup>6</sup>, X.R. Zhou<sup>59,73</sup>, X.Y. Zhou<sup>40</sup>, Y.X. Zhou<sup>79</sup>, Y.Z. Zhou<sup>12,e</sup>, A.N. Zhu<sup>65</sup>, J. Zhu<sup>44</sup>, K. Zhu<sup>1</sup>, K.J. Zhu<sup>1,59,65</sup>, K.S. Zhu<sup>12,e</sup>, L. Zhu<sup>35</sup>, L.X. Zhu<sup>65</sup>, S.H. Zhu<sup>72</sup>, T.J. Zhu<sup>12,e</sup>, W.D. Zhu<sup>12,e</sup>, W.J. Zhu<sup>1</sup>, W.Z. Zhu<sup>20</sup>, Y.C. Zhu<sup>59,73</sup>, Z.A. Zhu<sup>1,65</sup>, X.Y. Zhuang<sup>44</sup>, J.H. Zou<sup>1</sup>, J. Zu<sup>59,73</sup>

<sup>1</sup> Institute of High Energy Physics, Beijing 100049, People's Republic of China

<sup>2</sup> Beihang University, Beijing 100191, People's Republic of China

<sup>3</sup> Bochum Ruhr-University, D-44780 Bochum, Germany

<sup>4</sup> Budker Institute of Nuclear Physics SB RAS (BINP), Novosibirsk 630090, Russia

<sup>5</sup> Carnegie Mellon University, Pittsburgh, Pennsylvania 15213, U.S.A.

<sup>6</sup> Central China Normal University, Wuhan 430079, People's Republic of China

<sup>7</sup> Central South University, Changsha 410083, People's Republic of China

<sup>8</sup> China Center of Advanced Science and Technology, Beijing 100190, People's Republic of China

<sup>9</sup> China University of Geosciences, Wuhan 430074, People's Republic of China

- <sup>10</sup> *Chung-Ang University, Seoul, 06974, Republic of Korea*
- <sup>11</sup> *COMSATS University Islamabad, Lahore Campus, Defence Road, Off Raiwind Road, 54000 Lahore, Pakistan*
- <sup>12</sup> *Fudan University, Shanghai 200433, People's Republic of China*
- <sup>13</sup> *GSI Helmholtzcentre for Heavy Ion Research GmbH, D-64291 Darmstadt, Germany*
- <sup>14</sup> *Guangxi Normal University, Guilin 541004, People's Republic of China*
- <sup>15</sup> *Guangxi University, Nanning 530004, People's Republic of China*
- <sup>16</sup> *Guangxi University of Science and Technology, Liuzhou 545006, People's Republic of China*
- <sup>17</sup> *Hangzhou Normal University, Hangzhou 310036, People's Republic of China*
- <sup>18</sup> *Hebei University, Baoding 071002, People's Republic of China*
- <sup>19</sup> *Helmholtz Institute Mainz, Staudinger Weg 18, D-55099 Mainz, Germany*
- <sup>20</sup> *Henan Normal University, Xinxiang 453007, People's Republic of China*
- <sup>21</sup> *Henan University, Kaifeng 475004, People's Republic of China*
- <sup>22</sup> *Henan University of Science and Technology, Luoyang 471003, People's Republic of China*
- <sup>23</sup> *Henan University of Technology, Zhengzhou 450001, People's Republic of China*
- <sup>24</sup> *Huangshan College, Huangshan 245000, People's Republic of China*
- <sup>25</sup> *Hunan Normal University, Changsha 410081, People's Republic of China*
- <sup>26</sup> *Hunan University, Changsha 410082, People's Republic of China*
- <sup>27</sup> *Indian Institute of Technology Madras, Chennai 600036, India*
- <sup>28</sup> *Indiana University, Bloomington, Indiana 47405, U.S.A.*
- <sup>29a</sup> *INFN Laboratori Nazionali di Frascati, I-00044, Frascati, Italy*
- <sup>29b</sup> *INFN Sezione di Perugia, I-06100, Perugia, Italy*
- <sup>29c</sup> *University of Perugia, I-06100, Perugia, Italy*
- <sup>30a</sup> *INFN Sezione di Ferrara, I-44122, Ferrara, Italy*
- <sup>30b</sup> *University of Ferrara, I-44122, Ferrara, Italy*
- <sup>31</sup> *Inner Mongolia University, Hohhot 010021, People's Republic of China*
- <sup>32</sup> *Institute of Modern Physics, Lanzhou 730000, People's Republic of China*
- <sup>33</sup> *Institute of Physics and Technology, Mongolian Academy of Sciences, Peace Avenue 54B, Ulaanbaatar 13330, Mongolia*
- <sup>34</sup> *Instituto de Alta Investigación, Universidad de Tarapacá, Casilla 7D, Arica 1000000, Chile*
- <sup>35</sup> *Jilin University, Changchun 130012, People's Republic of China*
- <sup>36</sup> *Johannes Gutenberg University of Mainz, Johann-Joachim-Becher-Weg 45, D-55099 Mainz, Germany*
- <sup>37</sup> *Joint Institute for Nuclear Research, 141980 Dubna, Moscow region, Russia*
- <sup>38</sup> *Justus-Liebig-Universität Giessen, II. Physikalisches Institut, Heinrich-Buff-Ring 16, D-35392 Giessen, Germany*
- <sup>39</sup> *Lanzhou University, Lanzhou 730000, People's Republic of China*
- <sup>40</sup> *Liaoning Normal University, Dalian 116029, People's Republic of China*
- <sup>41</sup> *Liaoning University, Shenyang 110036, People's Republic of China*
- <sup>42</sup> *Nanjing Normal University, Nanjing 210023, People's Republic of China*
- <sup>43</sup> *Nanjing University, Nanjing 210093, People's Republic of China*
- <sup>44</sup> *Nankai University, Tianjin 300071, People's Republic of China*
- <sup>45</sup> *National Centre for Nuclear Research, Warsaw 02-093, Poland*
- <sup>46</sup> *North China Electric Power University, Beijing 102206, People's Republic of China*
- <sup>47</sup> *Peking University, Beijing 100871, People's Republic of China*
- <sup>48</sup> *Qufu Normal University, Qufu 273165, People's Republic of China*
- <sup>49</sup> *Renmin University of China, Beijing 100872, People's Republic of China*
- <sup>50</sup> *Shandong Normal University, Jinan 250014, People's Republic of China*
- <sup>51</sup> *Shandong University, Jinan 250100, People's Republic of China*
- <sup>52</sup> *Shanghai Jiao Tong University, Shanghai 200240, People's Republic of China*
- <sup>53</sup> *Shanxi Normal University, Linfen 041004, People's Republic of China*
- <sup>54</sup> *Shanxi University, Taiyuan 030006, People's Republic of China*
- <sup>55</sup> *Sichuan University, Chengdu 610064, People's Republic of China*
- <sup>56</sup> *Soochow University, Suzhou 215006, People's Republic of China*

- <sup>57</sup> *South China Normal University, Guangzhou 510006, People's Republic of China*
- <sup>58</sup> *Southeast University, Nanjing 211100, People's Republic of China*
- <sup>59</sup> *State Key Laboratory of Particle Detection and Electronics, Beijing 100049, Hefei 230026, People's Republic of China*
- <sup>60</sup> *Sun Yat-Sen University, Guangzhou 510275, People's Republic of China*
- <sup>61</sup> *Suranaree University of Technology, University Avenue 111, Nakhon Ratchasima 30000, Thailand*
- <sup>62</sup> *Tsinghua University, Beijing 100084, People's Republic of China*
- <sup>63a</sup> *Istinye University, 34010, Istanbul, Turkey*
- <sup>63b</sup> *Near East University, Nicosia, North Cyprus, 99138, Mersin 10, Turkey*
- <sup>64</sup> *University of Bristol, H H Wills Physics Laboratory, Tyndall Avenue, Bristol, BS8 1TL, U.K.*
- <sup>65</sup> *University of Chinese Academy of Sciences, Beijing 100049, People's Republic of China*
- <sup>66</sup> *University of Groningen, NL-9747 AA Groningen, The Netherlands*
- <sup>67</sup> *University of Hawaii, Honolulu, Hawaii 96822, U.S.A.*
- <sup>68</sup> *University of Jinan, Jinan 250022, People's Republic of China*
- <sup>69</sup> *University of Manchester, Oxford Road, Manchester, M13 9PL, U.K.*
- <sup>70</sup> *University of Muenster, Wilhelm-Klemm-Strasse 9, 48149 Muenster, Germany*
- <sup>71</sup> *University of Oxford, Keble Road, Oxford OX13RH, U.K.*
- <sup>72</sup> *University of Science and Technology Liaoning, Anshan 114051, People's Republic of China*
- <sup>73</sup> *University of Science and Technology of China, Hefei 230026, People's Republic of China*
- <sup>74</sup> *University of South China, Hengyang 421001, People's Republic of China*
- <sup>75</sup> *University of the Punjab, Lahore-54590, Pakistan*
- <sup>76a</sup> *University of Turin, I-10125, Turin, Italy*
- <sup>76b</sup> *University of Eastern Piedmont, I-15121, Alessandria, Italy*
- <sup>76c</sup> *INFN, I-10125, Turin, Italy*
- <sup>77</sup> *Uppsala University, Box 516, SE-75120 Uppsala, Sweden*
- <sup>78</sup> *Wuhan University, Wuhan 430072, People's Republic of China*
- <sup>79</sup> *Yantai University, Yantai 264005, People's Republic of China*
- <sup>80</sup> *Yunnan University, Kunming 650500, People's Republic of China*
- <sup>81</sup> *Zhejiang University, Hangzhou 310027, People's Republic of China*
- <sup>82</sup> *Zhengzhou University, Zhengzhou 450001, People's Republic of China*

<sup>a</sup> *Also at the Novosibirsk State University, Novosibirsk, 630090, Russia*

<sup>b</sup> *Also at State Key Laboratory of Nuclear Physics and Technology, Peking University, Beijing 100871, People's Republic of China*

<sup>c</sup> *Also at MOE Frontiers Science Center for Rare Isotopes, Lanzhou University, Lanzhou 730000, People's Republic of China*

<sup>d</sup> *Also at Lanzhou Center for Theoretical Physics, Lanzhou University, Lanzhou 730000, People's Republic of China*

<sup>e</sup> *Also at Key Laboratory of Nuclear Physics and Ion-beam Application (MOE) and Institute of Modern Physics, Fudan University, Shanghai 200433, People's Republic of China*

<sup>f</sup> *Also at School of Physics and Electronics, Hunan University, Changsha 410082, China*

<sup>g</sup> *Also at the Moscow Institute of Physics and Technology, Moscow 141700, Russia*

<sup>h</sup> *Also at Guangdong Provincial Key Laboratory of Nuclear Science, Institute of Quantum Matter, South China Normal University, Guangzhou 510006, China*

<sup>i</sup> *Also at Hangzhou Institute for Advanced Study, University of Chinese Academy of Sciences, Hangzhou 310024, China*

<sup>j</sup> *Also at Goethe University Frankfurt, 60323 Frankfurt am Main, Germany*

<sup>k</sup> *Also at the Department of Mathematical Sciences, IBA, Karachi 75270, Pakistan*

<sup>l</sup> *Currently at Silesian University in Katowice, Chorzow, 41-500, Poland*

<sup>m</sup> *Also at the NRC "Kurchatov Institute", PNPI, 188300, Gatchina, Russia*

<sup>n</sup> *Also at Ecole Polytechnique Federale de Lausanne (EPFL), CH-1015 Lausanne, Switzerland*

<sup>o</sup> Also at Key Laboratory for Particle Physics, Astrophysics and Cosmology, Ministry of Education;  
Shanghai Key Laboratory for Particle Physics and Cosmology; Institute of Nuclear and Particle Physics,  
Shanghai 200240, People's Republic of China

<sup>p</sup> Also at Helmholtz Institute Mainz, Staudinger Weg 18, D-55099 Mainz, Germany

<sup>†</sup> Deceased